Westinghouse Electric Corporation
AEROSPACE DIVISION

Friendship International Airport
Box ... Baltimore ... Md
Telephone ...

September 18, 1964

A1819AU

Advanced Plans and Programs Division (ASZ-5)
Deputy for Systems Management
Hq., Aeronautical Systems Division
Wright-Patterson Air Force Base, Ohio

Subject: Contract AF33(657)13264
Westinghouse Reference AAD-51244

Enclosure (1): Three (3) copies Progress Report for Contract AF33(657)13264 for Period 18 September 1964 - 30 August 1964.

Gentlemen:

In accordance with the subject contract, Enclosure (1) is submitted. A copy of this report is also being sent to the Technical Director.

Very truly yours,

WESTINGHOUSE ELECTRIC CORPORATION

R. W. Eby
Marketing Specialist
Marketing Department

RWE:sb

Document No. X-257

Copy 4 of 5

Pages i through viii
and 1 through 108

THALO ACTIVE SYSTEM

Progress Report #1

For Period

18 January 1964 through 30 August 1964

AF 33(657)-13264

15 September 1964

Westinghouse Defense and Space Center
Aerospace Division
Baltimore, Maryland

TABLE OF CONTENTS

Paragraph		Page
1.	Introduction and Summary	
1.1	Introduction	1
1.2	Establishment of Tasks	1
1.3	Major Events	2
1.4	Contract Costs	3
1.5	Project Tasks	3
1.5.1	Anticipatory Costs	3
1.5.2	Administration	5
1.5.3	Project System Analysis	6
1.6	Systems Analysis	7
1.6.1	Frequency Choice	7
1.6.2	Target Characteristics	10
1.6.3	Antenna Coverage	12
1.6.3.1	Gain Pattern Investigation	13
1.6.3.2	Pointing Angle and Beamwidth Pointing Investigation	14
1.6.3.3	Summary	16
1.6.4	Integration Time	16
1.6.5	Filter Bank Parameters	17
1.6.6	PRF and Duty Cycle	22
1.6.7	Signal/Noise	22
1.6.8	System Mechanization	24
1.6.9	Miscellaneous Analyses	26
1.6.10	Clutter Spectrum Considerations	27
1.6.11	Table of Parameters	29

TABLE OF CONTENTS (continued)

Paragraph	Page
1.7 System Configuration	35
1.7.1 Antenna	35
1.7.2 Radar Electronics	36
1.7.3 Cooling System	38
1.8 Clutter Flight Test Program	39
1.8.1 Purpose	39
1.8.2 General Description	39
1.8.3 Equipment	40
1.8.4 Procedures	40
2. Active Subsystem Mechanization and Integration	
2.1 Mechanization and Sequence of Operation	45
2.1.1 Present System Mechanization	46
2.1.2 Frequency Diversity and Jam Avoidance	51
2.1.3 Sequence of Operation	51
2.2 Transmitter and RF Circuits	56
2.2.1 Crystal Oscillator Stability	58
2.2.2 Solid State Power Amplifier	61
2.2.3 Final RF Amplifier	64
2.2.3.1 Tuned Line Deformation	66
2.2.4 Duplexer	68
2.2.5 High Power Limiter	71
2.2.6 High Voltage Power Supplies	72
2.3 Receiver	73
2.3.1 Preselector	73

TABLE OF CONTENTS (continued)

Paragraph	Page
2.3.1.1 Cross Modulation	73
2.3.1.2 Intermodulation	75
2.3.1.3 Noise Figure	77
2.3.2 Second IF Converter	78
2.3.3 Main IF Amplifier and Converter	80
2.4 Data Processor	83
2.4.1 System Operation Sequencing	83
2.4.1.1 Data Processor Functional Operations	83
2.4.1.1.1 Timing Signals	83
2.4.1.1.2 Selection of Transmitter Frequency	85
2.4.1.1.3 Processing of Threshold Detection	85
2.4.1.1.4 Alarm	89
2.4.1.1.5 Velocity Multiplier Amplifier Control (VMAC)	89
2.4.2 Mechanization	90
2.4.2.1 Circuits	90
2.4.2.2 Packaging	90
2.4.3 Progress to Date	90
2.5 Clutter Tracker and Video Circuits	92
2.5.1 Clutter Tracker Mechanization	92
2.5.2 Clutter Tracker-Navigator Interface	92
2.5.3 Velocity Track VCXO	93
2.5.4 Velocity Multiplier	94
2.5.5 Scan VCXO	94
2.5.6 Fixed Oscillator	94

TABLE OF CONTENTS (continued)

Paragraph		Page
2.5.7	Mixers	94
2.5.8	Clutter Spectrum	95
2.5.9	Gating Circuits	95
2.6	Low Voltage Power Supplies and Special Test Equipment	96
2.6.1	Low Voltage Power Supplies	96
2.6.1.1	Design Changes Since Proposal	96
2.6.1.2	Description and Characteristics	98
2.6.1.3	Present Status of Low Voltage Power Supplies	99
2.6.2	Special Test Equipment	99
2.7	Filter Bank and Interrogator	100
2.7.1	Channelization of the Doppler Spectrum	100
2.7.2	Envelope Detection and Integration	101
2.7.3	Commutation or Interrogation	102
2.8	Active Subsystem Plans for Next Reporting Period	104
	3. Antenna Subsystem	
3.1	Analysis and Model Study	105
3.1.1	Analysis	105
3.1.2	Model Study - Traveling Wave Antenna	105
3.1.3	Plans for Next Reporting Period, Analysis and Model Study	107
3.2	Development of Elements and Power Dividers	107
3.2.1	Radiating Elements	108
3.2.2	Power Dividers	108
3.2.3	Plans for Next Reporting Period, Elements and Power Dividers	108
3.3	Fabrication and Test of Deliverable Antenna System	108

LIST OF ILLUSTRATIONS

Figure		Page
1-1	Required and Expected Gain Patterns	15
1-2	Number of Whole Looks for "Worst" Target	18
1-3	Acceptance Acceleration Band	20
1-4	Required Two Way Antenna Gain (db)	23
1-5	σ_o vs Frequency Over Water	28
1-6	Clutter Flight Test System Block Diagram	42
1-7	System Configuration For Calibration	43
2-1	Radar Block Diagram (Obsolete)	47
2-2	Radar Block Diagram (Current)	48
2-3	Left-Right Amplitude Comparator	50
2-4	Sequence of Operations in a Jammed Environment (No Echos)	52
2-5	Sequence of Operations for One Hit or Two Hits	53
2-6	Sequence of Operations Timing Diagram	54
2-7	Transmitter Block Diagram	57
2-8	Test Arrangement for Measurement of FM Sidebands	60
2-9	Sensitivity of 30 mc Crystal Oscillator to Vibration Stress	62
2-10	Sensitivity of 30 mc Crystal Oscillator to Power Supply Ripple	63
2-11	Solid State Power Amplifier	65
2-12	Maximum Sideband Amplitude with Respect to Carrier Under Eccentric Deformation	69
2-13	FM Sideband Amplitude with Respect to Carrier Under Line Length Variations	70
2-14	Preselector	74
2-15	Pulse Decay in Preselector Filter	76
2-16	Second IF Converter	79

LIST OF ILLUSTRATIONS (continued)

Figure		Page
2-17	Main IF Amplifier and Converter	81
2-18	System Operation Sequencing	84
2-19	Data Processor Functional Block Diagram	87
2-20	Target Criteria	88
2-21	Power Distribution Wiring with Multiple Power Supplies Feeding into the Same Unit	97
2-22	Power Distribution Wiring with One Power Supply Feeding into Multiple Units	97
3-1	Traveling Wave Antenna	106

Approved For Release 2001/08/28 : CIA-RDP67B00657R000200260001-7
SPECIAL HANDLING

LIST OF TABLES

Table		Page
1-1	Summary Table of System Parameters	8
1-2	Table of Radar Parameters	30
1-3	System Weight, Volume and Power	37
2-1	Transmitter Parameters	56
2-2	Data Processor Board Divisions	91

SPECIAL HANDLING

Approved For Release 2001/08/28 : CIA-RDP67B00657R000200260001-7

1. INTRODUCTION AND SUMMARY

1.1 INTRODUCTION

This is the first informal monthly technical report under Contract AF 33(657)-13264 and covers the period from January 17 through August 30, 1964. None prior to this report has been published as considerable effort has been devoted to system analysis, and system parameters of this project have changed rapidly. However, close personal liaison has been maintained with the Project Engineer and other members of the customer's technical staff in resolving these parameter changes and in maintaining up-to-date knowledge of project status.

Now, sufficient progress has been made in the analysis of the active sub-system to document the decisions which have been reached and to render informal monthly reports upon technical progress and additional system changes which may occur. To accomplish this requires a more detailed report, at this time, than is contemplated for the usual informal monthly technical report.

1.2 ESTABLISHMENT OF TASKS

In order to establish technical and administrative control of the contract, the work being performed thereunder has been divided into tasks. These have been grouped in three major categories:

a. Project

b. Active Subsystem

c. Antenna Subsystem

Included under Project tasks are:

a. Project administration

b. System analysis

c. Clutter flight test program

Included under Active Subsystem tasks are:

a. Active Subsystem Mechanization and Integration

b. Transmitter and RF circuits

c. Receiver

d. Data processing

e. Clutter Tracker and Video circuits

f. Low Voltage Power Supplies and Special Test Equipment

g. Filter Bank and Interrogator

Included under Antenna Subsystem tasks are:

a. Analysis and Model Study

b. Development of Elements and Power Dividers

c. Fabrication and Test of Deliverable Antenna System

For this and subsequent monthly technical reports, project efforts will be reported by tasks under these major categories.

1.3 MAJOR EVENTS

In summary, the major events, which have occurred during the period herein reported, are tabulated below:

a. Preliminary system Analysis (performed intermittently from the issuance of the initial proposal January 18, 1964 until verbal authorization to proceed was given April 8, 1964. This was a limited effort for which anticipatory costs have been allowed).

b. Requote of active subsystem and quote for antenna subsystem on or about April 7, 1964.

c. Continued system analysis (April 8, 1964 to present date).

d. Requote of antenna subsystem May 8, 1964.

e. Receipt of letter contract, May 15, 1964.

f. Analysis of anticipated radio frequency interference to operation and its effect upon operating frequency power. (This analysis resulted in a decision on or about June 22, 1964, to change the operating frequency from that proposed January 18, 1964 and to double the operating power and the consequent increase in the scope of work outlined in document A18122U, dated July 2, 1964).

g. Mechanization study, definition of subunits and preliminary subunit design (April 8, 1964 to present date)

h. Receipt of definitive contract and first amendment thereto, August 11, 1964.

1.4 CONTRACT COSTS

The costs incurred under this contract are reported separately and are not included within this report.

1.5 PROJECT TASKS

1.5.1 Anticipatory Costs

Initially the anticipatory costs were considered to be those accrued prior to verbal contract go-ahead on April 8, 1964. This effort was devoted to continuing system analysis from January 18, 1964,

with the primary purpose of establishing firm system parameters. Additional effort was devoted toward system mechanization. A preliminary block diagram was developed and from this block diagram preliminary sub-unit definitions were made. Further technical effort was devoted toward investigation of clutter filters, filter banks and preparation of technical data demonstrating that the performance required of these filters is achievable in the operating environment in which operation is intended.

The total costs so accrued and charged to engineering task AA1A are approximately $19,100, of which approximately $1,100 costs relate to the passive system electronics and will be transferred to contract AF33(657)13262 which resulted from that effort and $3000 of which costs relate to the passive antenna system and will be transferred to contract AF33(657)13261. The $15,000 remaining costs relate to the active subsystem and make up the anticipatory costs allowed under Contract AF33(657)13264.

However, under the definitive contract issued August 11, 1964, anticipatory costs are defined as those accrued prior to May 26, 1964. Therefore, anticipatory costs, so defined, consist of time and materials accrued against engineering tasks other than AA1A between April 8, 1964 and May 26, 1964, plus the $15,000 determined above. Engineering Task AA1A was closed April 8, 1964, and no costs were accrued to it subsequent to April 8, 1964. Thus, under the contract definition, total "anticipatory costs" to May 26, 1964, for Contract AF33(657)13264 are approximately $100,000.

Note: that all references to costs made above are based upon

engineering department computations and are not official. Official computations must come from the Accounting Department.

1.5.2. Administration

A small project group has been established for administrative and technical control of this project, the persons named below serve full time on the project:

a. F. G. Mullins as Program Manager and primary Westinghouse representative.

b. H. S. Murray, Senior Engineer, as assistant to the program manager, responsible for engineering cost and schedule control, technical reports, project security and other administrative aspects of the project.

c. J. W. Hughes, Senior Engineer, as assistant to the project manager, responsible for mechanical coordination of the project and mechanical liaison with the customer and with other contractors, responsible for related systems.

This project group serves the same functions with regard to contracts AF33(657)13261 and AF33(657)13262.

In addition, J. W. Stuntz, Manager Aerospace Development Engineering; H. B. Smith, Aerospace Engineering Manager; N. V. Petrou, VP and General Manager, Aerospace Division and R. W. Eby, Aerospace Marketing Project Liaison, function with the project group on a part-time basis in their respective capacities, as required.

1.5.3. Project System Analysis

Also serving the project, since its beginning and at the present time upon an essentially full time basis, are D. H. Mooney, Advisory Engineer, radar systems specialist, and M. S. Wheeler, Advisory Engineer, Antenna Systems specialist. These have primary technical responsibility for the establishment of system operating parameters and equipment specifications for a system fulfilling the operating requirements established by the customer.

1.6 SYSTEMS ANALYSIS

A considerable amount of effort during this reporting period has been devoted to more detailed analyses of system requirements, based on new and more complete customer input data. Furthermore, in a number of areas, ways have been devised which improve performance beyond that originally obtained. Also, a number of potential problems were uncovered which were not previously realized, and have been circumvented by modifying the mechanization.

1.6.1 Frequency Choice

The most important single analysis involved a study of the effect of transmitted frequency choice on the radar interference performance, detection performance, and hardware physical characteristics. Of these, the interference sources were by far the overriding consideration. The frequency band from 100-500 mc was studied, which includes TV, high power pulse radar, navigation aids, telemetry, and narrow-band communications interference sources. The original proposed choice of 190-200 mc fell in the TV band so a detailed analysis was made first of the possibility of operating in the vicinity of both on-frequency and off-frequency TV channels. To back up the analysis, spectral measurements were made at a local TV station. A map of the geographical area which would be negated by interference was prepared, and forcefully showed the hopelessness of such a frequency choice.

A similar study of operating in the vicinity of the known types of pulse radar was made, and the conclusions were similarly negative. (In both cases the studies took into account interference spectra, antenna patterns, range variations, radar frequency hopping, etc.)

TABLE 1-1
SUMMARY TABLE OF SYSTEM PARAMETERS
FOR SAME S/N AS PROPOSAL

Radio Frequency (MC/S)	Radiated Power (KW)	Prime Power (KW)	System Weight (Pounds)	Volume (Cu. Ft.)	Frequency Tuning (MC/S)
145	0.9	2.0	378 #	6.0	1.2
240	2.0	4.5	360 #	6.4	9
360	5.6	11.7	482 #	8.8	15

It was decided that the only practical choice was to select an operating band where the interference sources were less potent. Three such bands were selected at 145 mc, 240 mc, and 360 mc as being representative of the clearest regions known (respectively, a ham band, a telemetry band, and a communications band). Similar calculations of interference problems showed that with improved receiver design (to be discussed subsequently) and with 6-10 mc tunability, quite acceptable performance would result in any of these bands. Therefore, preliminary hardware designs at each of these frequencies were made to compare the detection performance, or more simply, to compare the hardware required to obtain the same performance. It was found that considerable differences did exist, as shown in Table 1-1. The low frequency system had the lowest power requirement and volume, but had an unacceptable frequency tunability due to antenna bandwidth limitations. The high frequency system had excellent bandwidth, but was very heavy and required excessive power. The 240 mc system was the best compromise, having adequate bandwidth, lowest weight, and moderate power requirements. Compared to the original proposed system, however, it is somewhat larger and heavier and requires more power. It was concluded that this is a small price to pay to gain the improvement in interference immunity, and so was recommended to the customer in June, 1964, and was accepted.

The system modifications which are required to be compatible with the new frequency are:

1. The transmitter average power must be doubled (to 2 KW) to make up for the smaller target cross-section and reduced antenna receiving aperture at the higher frequency.

2. The antenna installation becomes more difficult, and is not yet fully settled. It appears that the proposed symmetrical installation about the vehicle centerline may not be possible due to excessive spacing between antenna elements at the shorter wavelength. If this be so, the two rows of elements must be mounted on the same side of center, which causes more severe mechanical interference problems and which requires the addition of a metal ground plane behind the outboard elements with obvious disadvantages.

3. The receiver must incorporate RF filtering and a smoothly shaped bang-snuffer pulse to reject the interference signals. The filtering is required to limit the interference levels so that they do not drive the receiver stages non-linear, causing clutter spectrum spreading due to intermodulation. The snuffer pulse shaping is necessary to prevent spectrum aliasing of out-of-band interference which would spread into the filter bank passband.

With the possible exception of the antenna, none of these modifications presents any problem of consequence. The antenna problem is still being studied and more detail will be given later in this report.

1.6.2 Target Characteristics

Considerably more data has become available from the customer regarding target characteristics, much of which has affected the detailed selection of system parameters. The information obtained concerns measured data of target cross-section as a function of angles and frequency, computer plots of target velocity and acceleration versus time for two target models and a range of target variables, and a revised vehicle flight profile.

The target cross-section data is very encouraging in that it is near the assumed magnitude of the proposal and it does not vary significantly with aspect angles of $\pm 15^{o}$ from the nose, hence the non-fluctuating model appears justified.

For the proposal a calculation had been made of target reflection based upon an rms sum of all the applicable surface reflections. The value of 3 meter square was thus used at 200 mc.

As measurements became available, it was found that 3 meter square was indeed a good design number for 200 mc but a deep null existed at 170 mc and again at 340 mc.

This target data will be avilable for the next report showing that return is generally good in the 200 mc and 250 mc regions.

Another area of interest has been in radar return from the missile exhaust. While there is a large amount of information available, particularly from Stanford Research, the results appropriate to this situation must be inferred. The principal problem is the lack of measurements from the frontal aspect. There is an exhaust return having skin doppler velocity but its magnitude can only be estimated at 10 meter^2 $\pm$ 10 db. For this reason, this return has not been included in the design work.

The new data on target velocity and acceleration versus time contours also are encourgaging in that they are less severe than the original proposal assumed. These data were converted into the minimum detectable velocity and the time available for detection as a function of position within the desired coverage contour. The available time was found to have a minimum at the maximum cross-range corner of the contour of from 1.49 to 1.97 seconds, depending on the target model

assumed, or an average of 1.73 seconds. This is very helpful compared to the 1.3 seconds of the nominal for the proposal, and permits getting more looks (which were found to be necessary as will be discussed).

The new ground coverage contour is also slightly more favorable in that it is somewhat smaller than that assumed in the proposal. All of the system calculations, including the above times, are now based on this new contour.

1.6.3 Antenna Coverage

In the proposal the antenna pattern was assumed to be a fan beam shape. A transmitted azimuth beam-width of 90° and receive of 45° with a 20° elevation beam-width was considered. In the geometry of the problem, the antenna pointing angle in elevation was selected to be 22-1/2° below the horizon. The receive beams were squinted 22-1/2° either side of the vehicle axis.

To check the coverage of the required area, a detailed study of the gain pattern was performed. With this small elevation pointing angle, the pattern is distorted from a fan beam because the antenna operation is approaching endfire conditions.

As has been mentioned, consideration of a different antenna configuration was also required due to the frequency change. At the new transmitted frequency, the symmetrical configuration proposed could only be mechanized with a spacing of approximately one wavelength between the rows of the array. An asymmetrical configuration is needed to reach the desirable 0.5λ spacing.

1.6.3.1 <u>Gain Pattern Investigation</u>

Examination of the gain pattern of the array was accomplished by synthesizing the theoretical pattern from the array and element patterns known to be generated assuming a flat ground plane. The pattern was then projected onto the earth plane for comparison with the desired coverage area.

Two undesirable effects were noted in the one wavelength spacing case. First, the main lobe receive pattern beam-width was narrowed. This made satisfactory coverage of the required area more difficult.

The second effect was the appearance of a sidelobe, only 3 db down from the main lobe and located on the opposite side of the vehicle axis. Operation with such an existing sidelobe could nullify or confuse the angle sense of detections made by the system.

A similar examination of patterns for 0.9λ spacing was also conducted since it was considered possible to attain that spacing. The results were not significantly different, however.

Inspection of the element receive pattern, which is the prime cause of the beam-width change and sidelobe generation, revealed that a 0.5λ spacing is optimum. Therefore, the process of synthesizing gain patterns and comparing them with the desired coverage was repeated for this case. The wider beam-width eased the coverage problems and, as expected, the sidelobe level was reduced to a negligible factor. Because of these factors, the use of the 0.5λ spacing, i.e., the asymmetrical antenna configuration, appears most desirable for good system performance.

The asymmetrical configuration, however, introduces another factor into the problem. Installation of the array on this configuration

would cause both rows to be placed on a plane inclined 18° in roll. The resulting off-center transmit pattern is undesirable and the antenna patterns must be intentionally distorted in order to make them symmetrical about the vehicle axis. A planned variation in the element design will accomplish this and will be described later in this report.

Figure 1.1 shows one-half of the coverage area on the earth with 2-way gain contours superimposed. These contours were drawn for the $0.5\ \lambda$ separation array mounted on the inclined plane. The dotted contours on the figure are desired gain contours generated from detection probability and eclipsing loss considerations as described in a later paragraph. The figure shows that satisfactory coverage will be obtained with this antenna configuration.

Note that the contours in figure 1.1 are shown in db below two-way peak gain. The two-way peak gain of the antenna system has been calculated to be 25 db including all antenna losses. This has increased two db from the proposed value because of more precise pattern and beam-width information.

1.6.3.2 Pointing Angle and Beam-width Investigation

Pointing angles and beam-width were varied to determine the proper values throughout the gain pattern investigation. Some changes were required to reach the pattern shown in figure 1.1.

The transmitted azimuth beam-width remained 90°. The received value changed to 49°. In elevation, both receive and transmit beam-widths became $21\text{-}1/2^{\circ}$.

It should be noted that the beam-width figures quoted exist only as one-way figures. In the synthesis of the 2 dimensional, two-way

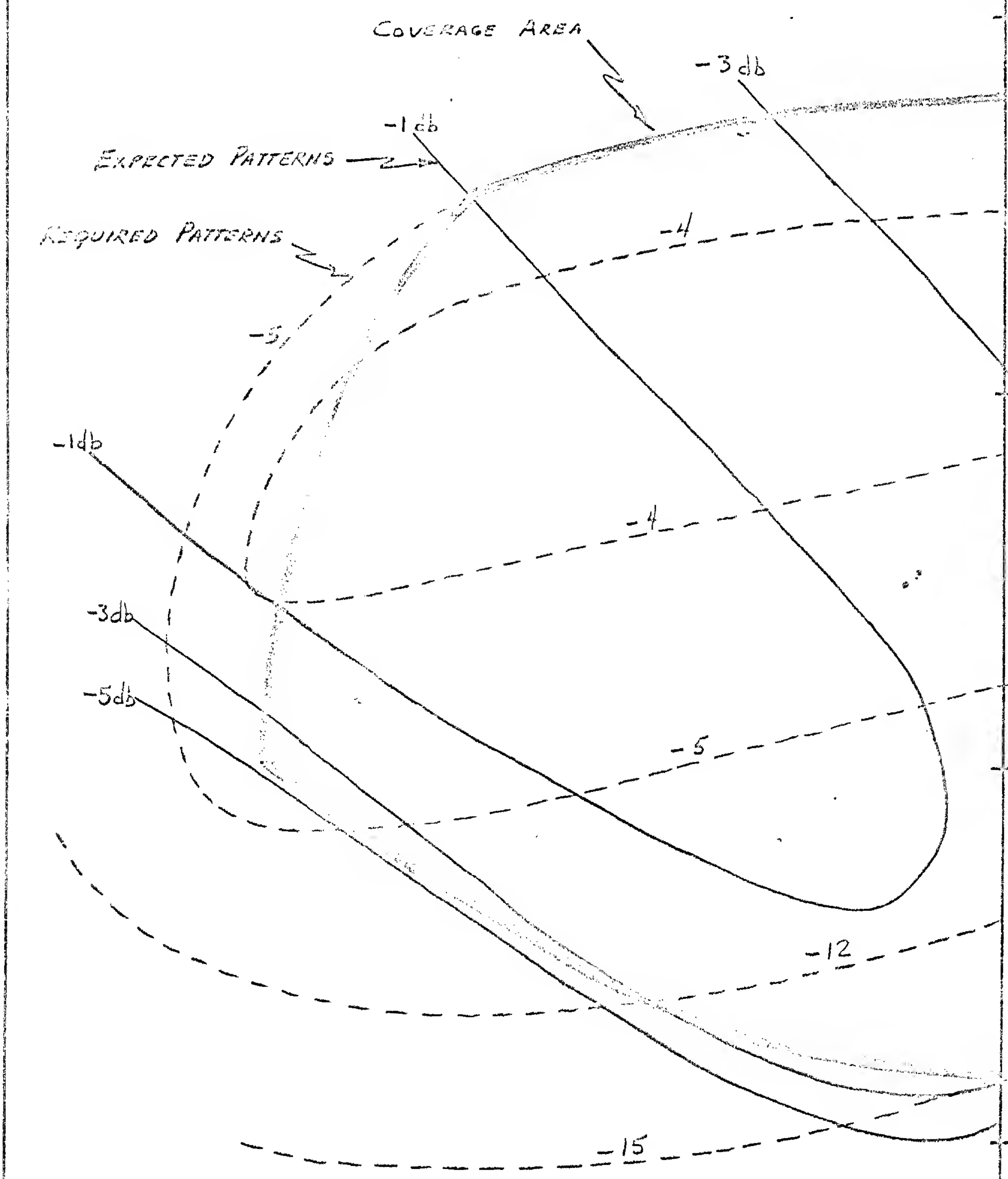

FIGURE 1-1 REQUIRED AND EXPECTED GAIN PATTERNS

patterns, due to the distortion near endfire, the azimuth and elevation planes are twisted so that one-plane dimensions lose their meaning.

Pointing angles both in azimuth and elevation were changed to optimize coverage. The depression angle measured from vehicle center line is 34^{o}, while a 20^{o} azimuth squint angle was selected.

1.6.3.3 Summary

Coverage investigations indicate that the space between rows of the array should be 0.5 λ for optimum coverage and complete absence of ambiguity. Present calculations are proceeding with the assumption that an asymmetrical antenna configuration must be used to reach this condition. It is possible that the alternate symmetrical form can be used if a method can be developed to shorten the electrical separation of the rows.

Use of the 0.5 λ spacing and the new pointing angles yields gain patterns which appear to satisfactorily cover the desired area.

1.6.4 Integration Time

Of all the parameters, other than the antenna, available for optimization, the selection of the integration time is probably the most important. There is only a short time available in which to make a detection, verify that it is a desired target, and reject undesired targets; in the meanwhile trying several PRF's so as to prevent eclipsing, and selecting the best transmitted frequency to minimize interference.

A study was made of the effect of integration time on the signal/noise required for detection. Shorter integration time is partly made up by having time for extra looks, but the longest possible time was always found to be best for detectability. When the effects of false

targets were considered, it was found that at least 4 looks are necessary to prevent possible missing of a true target due to the FHF switching sequences in the presence of a false target. Also, a study of the effect of having the radar looks not exactly synchronized with the target available time showed that a considerable loss resulted unless at least four look times are allowed for.

The integration time also influences the scanning loss that results when the true target acceleration does not exactly match the filter bank sweep rate. It also directly affects the filter bank movement of the target from one look to the next, and hence the discrimination performance. The former effect makes a short time desirable, while the latter makes a long time desirable. All of these effects were calculated and compared, and an integration time of 0.29 seconds was selected as the best compromise. This permits 4 looks as shown in figure 1.2 in virtually all cases, including even the worst of the target models, and reasonable performance in all the areas mentioned.

1.6.5 Filter Bank Parameters

The choice of filter bank parameters are also important in determining the detection and discrimination performance. The various effects were considered of the choice of band-width of the individual filter bank filters. The most important one is the discrimination capability between desired and false targets. The narrower the band-width, the greater the number of filters the target moves from look to look. An analysis of the centroiding error in determining the target average filter position showed that it would be at most $\pm$ 1/2 filter, corresponding to $\pm$ 1 filter increment error from look to look. Since this error is fixed, narrower filters improve discrimination.

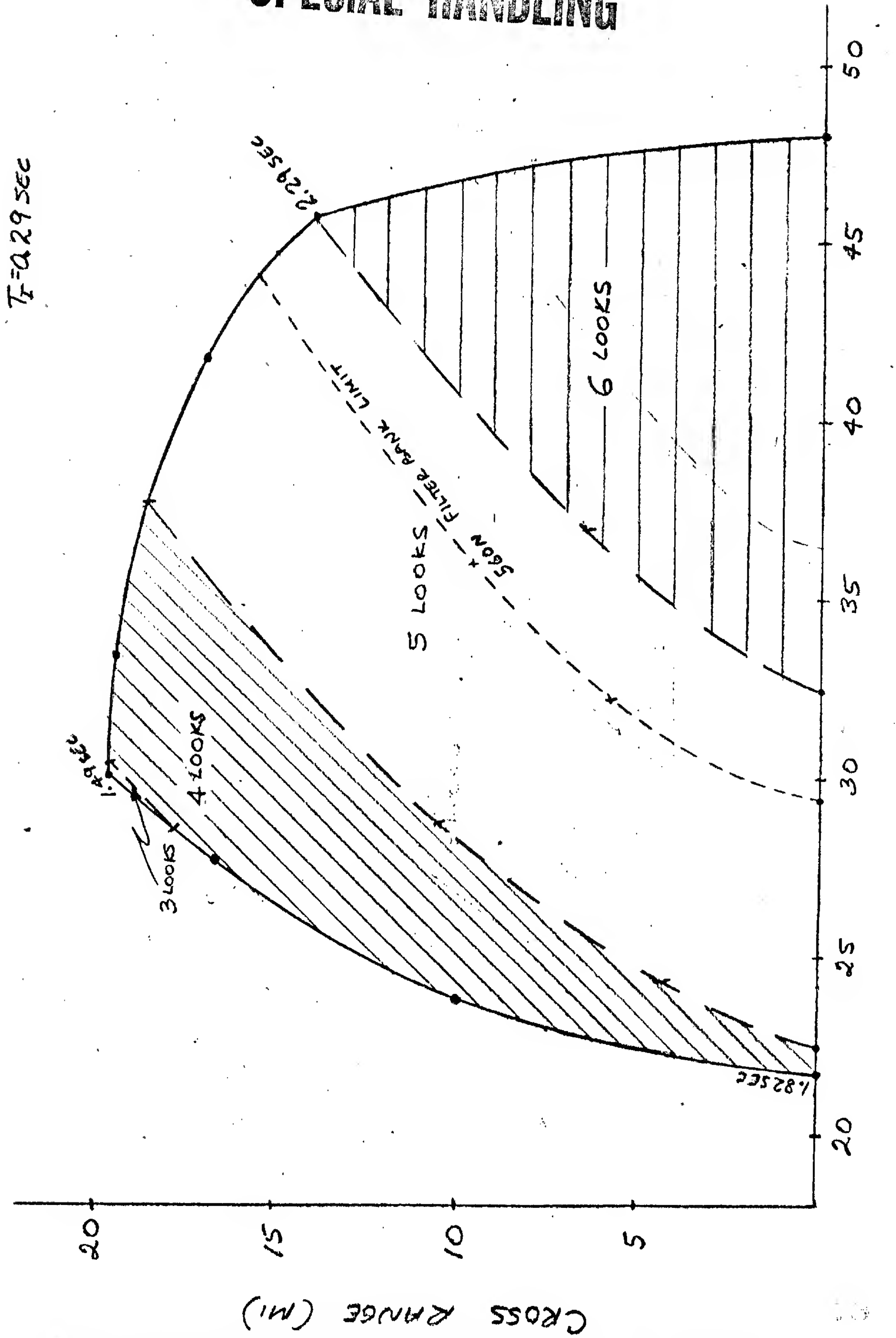

Figure 1-2 Number of Whole Looks for "Worst" Target

SPECIAL HANDLING

Narrow filters also slightly improve the S/N required for detection for a target which is stationary in the filter, but this is a minor effect due to the use of post detection integration. A serious problem would result, however, if too narrow filters were used, due to true targets which are not exactly matched to the filter bank scan. A scanning loss results due to shortened effective integration time. This is especially true for target signals that happen to fall near the split between two adjacent filters. Curves were made of this loss and the narrowest filters which gave acceptable loss were about 14 cps at the cross-over points. This choice results in the acceleration acceptance band of figure 1.3, due to centroiding errors, which seems quite reasonable. This figure is for the worst possible S/N and the average curve is much more nearly square.

The total band-width covered by the filter bank need at most cover from the clutter edge up to the highest target velocity of interest. It was found, however, that the upper edge is not at all critical, only affecting the maximum number of looks near zero azimuth. Beyond about 5 looks, very little is gained in detection performance, so the filter bank coverage was selected as 560 cps which gives at least 5 looks for all conditions of geometry. This reduces the number of filters somewhat below what would otherwise be needed, which is desirable due to the narrower filters now required.

The frequency response of the individual filter bank filters was originally a 2-pole Butterworth response. The effect of a very strong false target was found to be to trip off a very large number of filters, due to insufficient skirt attenuation. A study of maximum signal levels

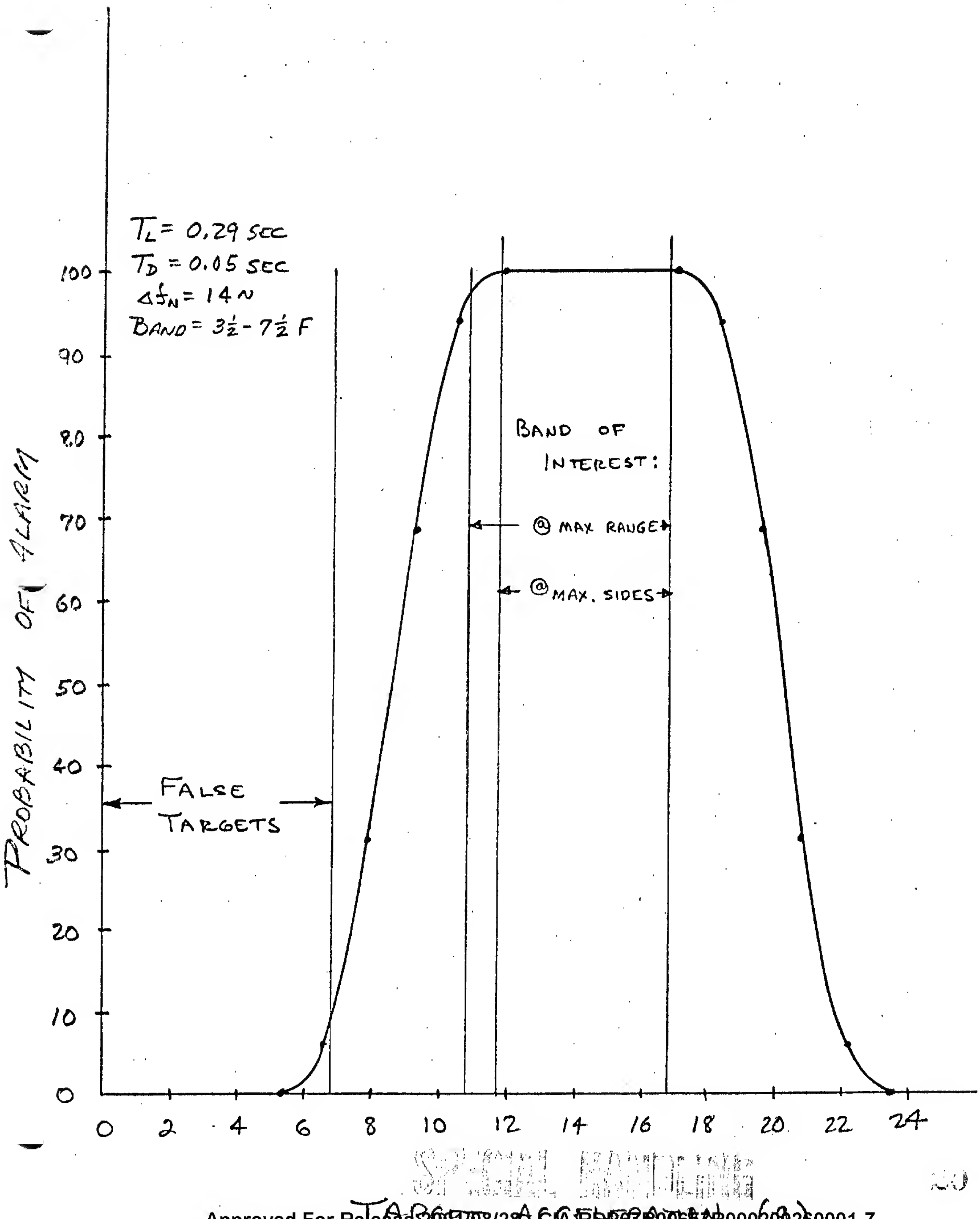

Figure 1-3 Acceptance Acceleration Band (at worst possible S/N)

and filter complexity resulted in the decision to go to 3-pole Butterworth filters, which limits the number of filters tripped to a value the digital centroiding circuits can handle, while also greatly reducing the portion of the filter bank which a false target can mask. These factors appear to definitely outweigh the additional complexity of the filters.

The optimum db point for one filter to cross-over an adjacent filter response was found to be less than the -3 db level originally assumed for two reasons. First, the detection performance is much poorer for a signal falling at this point, even though there are two filters which cumulate detection. Secondly, the filter bank mechanization can conserve on crystal elements by sharing them in adjacent filters, but the cross-over is then pre-determined and is -1.5 db for the 3-pole filters. This then was selected as the new cross-over to satisfy both desires, but, of course, is reflected in increasing the total number of filters.

In studying what is required to minimize the effect of interfering signals on the radar performance, it was found that a large dynamic range is desirable in the doppler amplifier right up to the filter bank. This restriction limits the gain which can be used ahead of the filters, and hence raises the gain required after each filter. This was found to be nearly 90 db of gain in each of 80 filters and, furthermore, each amplifier must be gain controllable for AGC and must track the others perfectly. This was concluded to be impractical so a filter bank mechanization was devised which uses only 1 amplifier which is time multiplexed between the 80 filters, hence getting perfect tracking. The hardware savings is small, however, since the switching circuits nearly make up for the amplifiers saved.

1.6.6 PRF and Duty Cycle

Two factors forced the PRF's to be increased over the proposed values. First, the doppler spread of targets increased due to the higher transmitted frequency, requiring a higher PRF to prevent ambiguity. Secondly, a new type of AGC was found to be necessary (to be discussed subsequently) which requires a clear band of doppler in which no target signals can appear. This requires raising the PRF even further. At the same time, it is desirable to select the PRF ratio so that bad eclipses are avoided, and to position those that remain to fall at ranges where the gain, range, and available time are not worst. As a result of such a study, the PRF's were selected as 7.42 KC and 6.36 KC, which satisfies all requirements.

The effect of transmitter duty cycle was also considered and it was found desirable to make the transmit pulse and receiver bang snuffer pulse duration equal. Because of a small dead time due to the ringing of the receiver RF interference filter, this turns out to be a transmitter duty cycle of about 0.48 rather than 1/2.

1.6.7 Signal/Noise

Because the antenna configuration is not completely firm at this time, rather than calculate the system detection performance for the actual antenna, the reverse has been done and the desired antenna pattern found for an assumed level of performance. Figure 1.4 shows the result of these calculations, over the ground coverage contour, to give 90% probability of detection (and discrimination) on the worst target model with the worst losses. In order to obtain this curve, all of the known losses in the signal processing had to be first evaluated, such as the scan loss due to the signal moving through the filter bank,

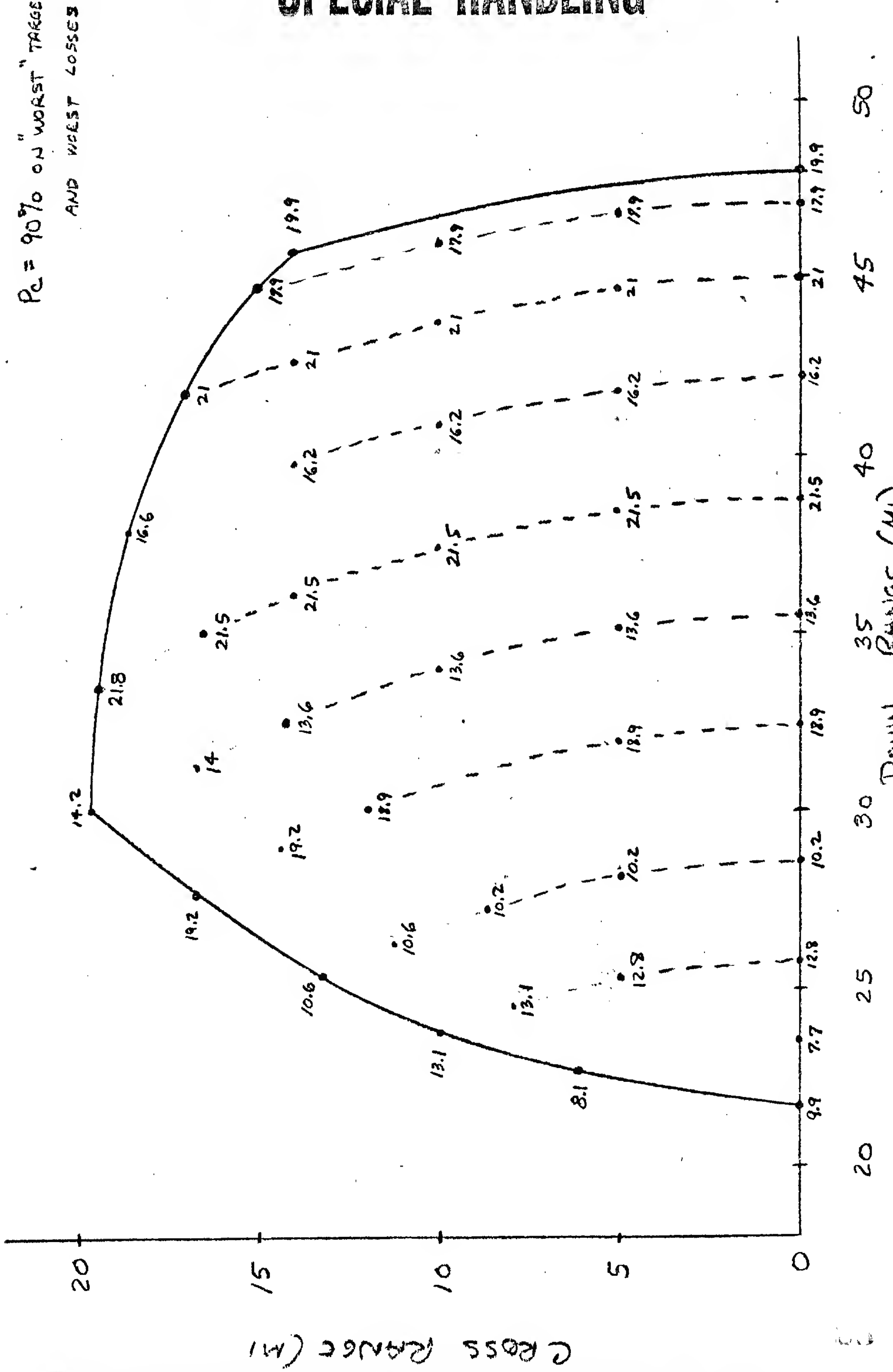

Figure 1-4 Required Two-Way Antenna Gain (db)

signal loss due to the signal falling at the filter bank cross-over point, misaligned looks relative to the target available time, etc. Also, the eclipsing was taken into account at each range, as well as the number of look times available.

Present indications are that the antenna can give at least these gains over the entire contour. The two regions which are most marginal, as expected, are the maximum cross range corner region of the coverage contour, and the maximum range, zero azimuth region. All other regions should have considerably better performance since the antenna gain margin will be greater.

In the process of calculating the S/N required for a given performance, a favorable error was found in the cumulation formulas given in the proposal for multiple looks and this was pointed out (and corrected) to the customer in an informal memo in February, 1964. Curves have been prepared for the per look and multiple look probabilities versus S/N for various conditions of eclipsing, and for various points on the filter bank filter response for the new system parameters.

1.6.8 System Mechanization

A number of mechanization trade-offs were considered which influence system performance independently of the hardware design. Several areas were found to give inadequate system performance and were subsequently modified accordingly. One of these was the AGC system, which was originally conceived as regulating the signal-plus-noise ahead of the filter bank, as past systems have done. This was concluded to be unacceptable in this system since strong false targets, as are likely to be present, can easily capture the AGC and submerge the desired targets.

Also, this arrangement is susceptible to interference pulses, causing coloration of the noise going into the filter bank. A new type of AGC system was devised, which operates on an out-of-band frequency region to prevent target suppression. By applying the AGC after the filter bank, coloration of the interference is prevented solving that problem too. The detection threshold was improved also by generating it from integrated noise, thereby cancelling component drifts.

The new AGC also eased the clutter filter requirements since clutter does not need to be completely rejected in the third IF anymore as it cannot affect the new AGC. The wider dynamic range ahead of the filter bank to minimize interference problems also eased the clutter filter requirements, since again the clutter need not be completely rejected. Both these effects combined make the clutter filter no longer a critical item.

Besides the new AGC, a new angle measurement mechanization has also been found to be desirable. The customer has stressed the need for reliable angle indication, since it apparently plays a crucial part of the alarm. As a result, the original mechanization has been modified to give a more reliable indication. The problem with the original is that a strong target can give both a "right" and "left" indication even though it is clearly left or right, by exceeding the threshold in both channels. A very simple modification has been made which now makes an amplitude comparison on a filter-by-filter basis each look, using a differential threshold. This will inhibit the wrong channel on strong targets, while still giving a "both" indication when the signals are approximately equal. (At the customer's request, only two indicator lights will be used rather than three, since "right" and "left" being

lit simultaneously can show "middle" adequately.) Performance of the improved angle measurement was calculated and found to be quite satisfactory, requiring about 3-4 db signal amplitude differential to operate.

1.6.9 Miscellaneous Analyses

A number of analyses were made to select the more detailed system parameters. For example, one covered the choice of IF frequencies and local oscillator frequencies for the receiver. Spurious signals can be very serious in a doppler radar unless very careful selection is made of the various frequencies. For example, each frequency must be chosen to avoid intermodulation products of all orders from falling in the pass bands and to avoid even very high harmonies of the radar PRF's. Such has been done and spurious frequencies should not be a problem.

Also, an analysis was made of the signal, clutter, and noise levels throughout the system since these influence the gain distribution and dynamic range desirable in the various bandwidth amplifiers.

The exact frequencies of known radio sources in the world in the band of interest were consulted in unclassified literature and exact transmitted frequencies selected so as to best cover the total system bandwidth while falling between the interference sources. A total of 7 frequencies were chosen as being adequate, an odd number being desirable for sequencing purposes.

A basically different type of "filter bank" mechanization was studied which appears to have some potential advantages in performance. This mechanization would use a magnetic tape recorder to record the doppler signals with a high speed read-head and a single multiplexed filter. A single filter would be adequate due to the time speed-up

of the read-head relative to write. Very steep and narrow filters could be easily implemented with this arrangement. Tape recorder suppliers were contacted and all agreed on feasibility, but none could deliver in the required time schedule. Therefore, the idea was dropped in preference to the original passive filter bank mechanization.

An analysis of the allowable frequency drift on each of the crystal oscillators in the system was made and in the endeavor, a mechanization was devised which completely cancels all drift in the first two local oscillators. In all cases the drift requirements are within the state of the art.

1.6.10 Clutter Spectrum Considerations

During the proposal stage, a value of reflection coefficient, σ_o, was used which had been developed by extrapolation of existing data. The clutter spectrum was predicted by manipulation of an idealized pattern incorporating the extrapolated σ_o.

In Section 1.6.3 antenna gain patterns are mentioned which were synthesized from known antenna parameters. These same patterns may be utilized to calculate the clutter spectrum more precisely than during the proposal phase. This work is now underway. Preliminary indications, using the extrapolated σ_o, are that clutter will be larger than predicted.

However, in the interim, some further data on reflectivity has been secured. Figure 1.5 shows a sample of this data. Values of σ_o are plotted versus frequency. The points above 1 Kmc were utilized in the proposal phase to predict the circled points at 415 mc in the proposal. Later data from studies done by NRL provided the boxed points at 428 mc.

SPECIAL HANDLING

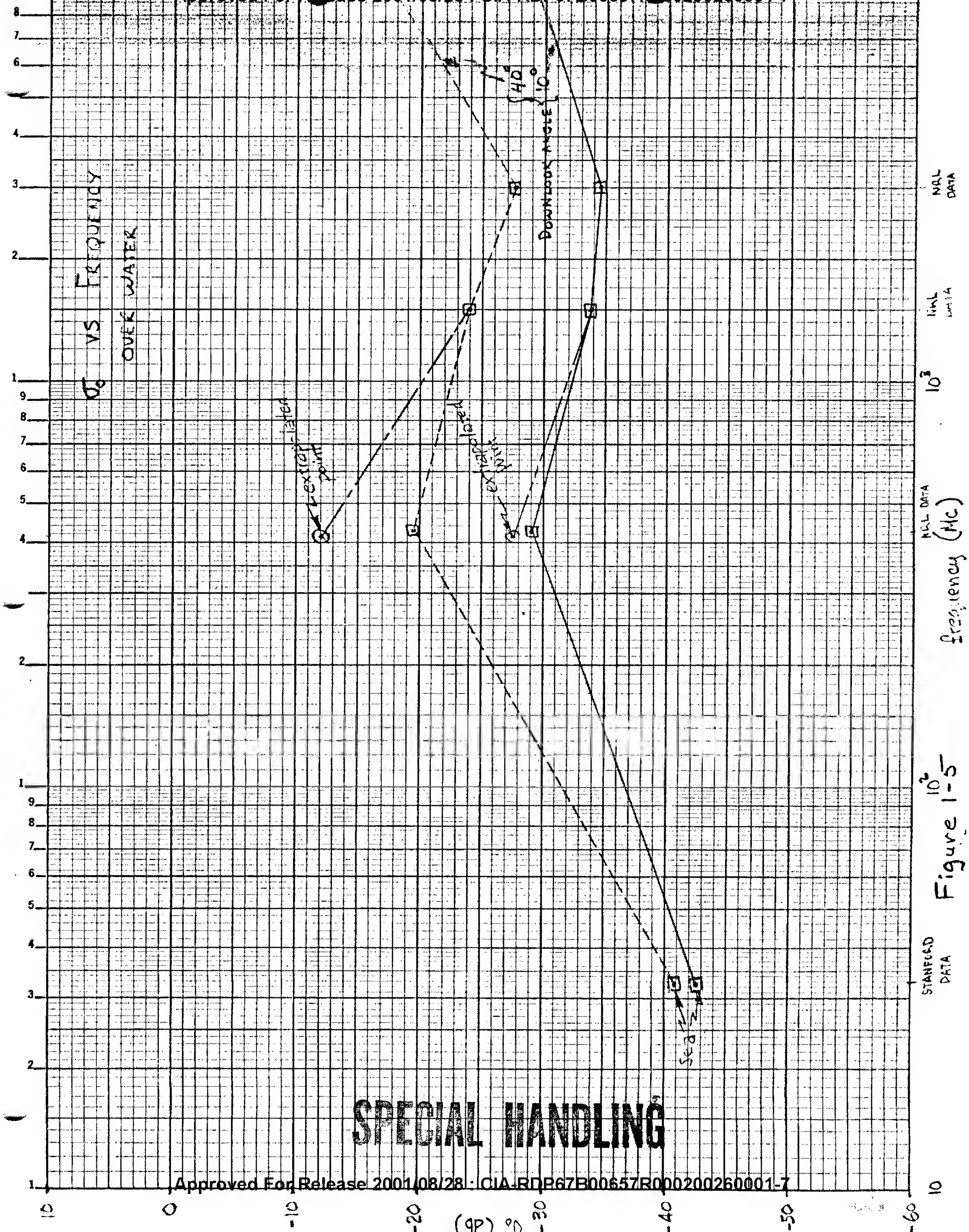

Figure 1-5

SPECIAL HANDLING

Approved For Release 2001/08/28 : CIA-RDP67B00657R000200260001-7

An investigation of backscatter performed by the Stanford Research Institute for the Office of Naval Research provided the data shown at 32.5 mc. If the linear extrapolation shown by the connecting lines were used, it would indicate that σ_o varies between -24 and -32 db at f_o. The proposal extrapolation predicted -12 to -28 db for the same down-look angles (40° and 10° respectively). Thus it appears that σ_o may be substantially lower than predicted. On the other hand, the linear extrapolation is of doubtful value, as evidenced by the slope variations seen on the curves. Also, little data was found on other types of terrain (Figure 1.5 is data taken over water) and ground targets should place more stringent requirements on the system.

In summary, new calculations on clutter indicate a higher level except that σ_o values may have decreased from the assumed. The ground clutter flight test (see Section 1.8) will shortly provide a value of σ_o which will settle the question. Final clutter spectrum levels and shape will be calculated as soon as the flight test data is available.

1.6.11 Table of Parameters

Because of the various factors discussed above, many of the radar parameters have been changed somewhat since the proposal was submitted in order to better optimize performance against the updated threat model. The present parameters are summarized in Table 1-2.

Table 1-2
Table of Radar Parameters

1.	Nominal transmitter frequency (f_o)	242.1 mc/s
2.	Number of selectable frequencies	7
3.	Spread of selectable frequencies	9 mc/s
4.	Exact transmitter frequencies:	-
	(1) f_o - 4.5 mc/s, (2) f_o - 3.5 mc/s, (3) f_o - 1.7 mc/s, (4) f_o - 0.2 mc/s, (5) f_o + 1.6 mc/s, (6) f_o + 3.5 mc/s, (7) f_o + 4.5 mc/s	
5.	Sequence of RF frequencies	1-4-7-3-6-2-5
6.	Average transmitted power	2 KW
7.	PRF's	(1) PRF #1 = 6.36 KC (2) PRF #2 = 7.42 KC
8.	PRF clock frequency	1,424,640 cps
9.	PRF dividers	(1) 32 x 7; (2) 32 x 6
10.	Transmitter pulse width	(1) 75.45 usec; (2) 64.25 usec
11.	Transmitter duty cycle	(1) 0.480; (2) 0.477
12.	Peak transmitted power	(1) 4.17 KW; (2) 4.20 KW
13.	Transmitter ON/OFF ratio	$\geq$ 125 db
14.	Number of receiver channels	2
15.	Receiver amplifier frequencies (clutter edge):	-
	RF amp	Transmit frequency
	First IF	29.112 mc/s
	Second IF	975.36 kc/s
	Third IF	84.96 kc/s
16.	Receiver amplifier bandwidths	-
	RF amp	5 mc/s
	First IF	5 kc/s
	Second If, Third IF	1.6 kc/s

17. Stalo crystal oscillator frequencies: -

    104.2445 mc/s; 104.7445 mc/s; 105.6445 mc/s;
    106.3945 mc/s; 107.2945 mc/s; 108.2445 mc/s;
    108.7445 mc/s

18. Second LO crystal oscillator frequency: - 28.13664 mc/s

19. Clutter track variable crystal oscillator frequency: - 975.36 kc/s (-) clutter edge freq.

20. Third LO variable crystal oscillator frequency: - 890.4 kc/s (+) filter bank sweep

21. Clutter track crystal oscillator frequency: 975.36 kc/s

22. Local oscillator frequencies: -

First LO	Transmit frequency (-) 29.111 mc/s
Second LO	28.13664 mc/s
Third LO	890.4 kc/s (+) filter bank sweep

23. Receiver amplifier gain: -

RF amp	15 db
First IF	0 db
Second IF	40 db
Third IF	70 db

24. Receiver internal noise figure ≤ 3 db

25. System noise temperature (at antenna terminals) $1{,}000^{\circ}$ K

26. Receiver sensitivity - 156 dbm

27. Maximum clutter/noise spectral density into receiver - 70 dbm

28. Maximum CW interference into receiver (3 mc spacing) - 32 dbm

29. Maximum input for 1 usec receiver recovery - 7 dbm

30. Maximum intermodulation products Equal to noise in 17 cps

31. Bang snuffer on-to-off ratio (2 stages) 50 db

32. Sloughing snuffer: -

Leading and trailing edge shape	$(\text{sine})^2$ per stage
Rise or fall time	4.2 usec

33. AGC dynamic range (2nd and 3rd IF)	70 db
34. Clutter track oscillator frequency offset control range:	
Linear	400-1,600 cps
Ground Test	0-1,600 cps
35. Clutter track oscillator stability and linearity:	-
	± 10 cps over range
36. Number of filter banks	2
37. Number of filters per filter bank	40
38. Filter bank bandwidth:	-
Cross-over	14 cps
- 3 db	16.2 cps
Noise	17 cps
39. Number of poles per filter	3 (Butterworth)
40. Total filter bank coverage	560 cps
41. Filter bank spacing from clutter edge (at sweep start)	100 cps
42. Filter bank sweep excursion	81 cps/0.34 sec
43. Post detection integration time	0.29 sec
44. Post detection integration samples (Marcum's N)	5
45. Receiver blanked time between looks:	-
PRF settle and AGC settle	0.1 sec
AGC settle only	0.05 sec
46. Total time per look:	-
No detection on previous look	0.39 sec
Detection on previous look	0.34 sec
47. False alarm number (Marcum's N)	10^6
48. False alarm time (average):	-
Per look (noise only)	15 minutes
Verified detection (noise only, two looks)	10^7 years
Verified detection (noise plus false target, two looks)	75 minutes

49.	Number of looks required for detection:	-
	True target only, at 50% - 50% eclipse	2
	True target only, at 0% - 100% eclipse	2-3
	False target at 0% - 100% eclipse, plus true target	2-4
	False target at 50% - 50% eclipse, plus true target	2-5
50.	Bank multiplex scan rate	6.36 kc/s
51.	Number of samples scanned	84
52.	Scanning sequence rate	75.7 cps
53.	Number of sequences per integration time	22
54.	Filter bank instantaneous dynamic range:	-
	Filter bank driver	40 db
	Filter bank multiplex amplifier	20 db
55.	Bandwidth of AGC filter	560 cps
56.	AGC range of filter bank multiplex amplifier	+ 10 to - 30 db
57.	Maximum number of filters exceeding threshold:	-
	Strong true target	3
	Strong false target	10
58.	True target look-to-look filter - centroid acceptable movement	+ 3-1/2 to + 7-1/2
59.	False target look-to-look filter - centroid rejection movement	- 3 to + 3
60.	Multiple target filter - centroid acceptable movement for inhibit	- 1-1/2 to + 1-1/2
61.	Angle quantizing	Right, left, both
62.	Alarm indication	Right light, left light, audio tone
63.	Alarm duration	30 seconds
64.	Navigation input data:	-
	Quantization	1 knot
	Maximum range	4,096 knots
	Data rate	1 sample/second

65. Power supply voltages and currents: -

+ 42 V @ 0.84 amps approx.
+ 22 V @ 1.72 amps approx.
+ 12 V @ 0.91 amps approx.
+ 6 V @ 2.49 amps approx.
+ 6 V @ 4.00 amps approx.
- 14 V @ 1.93 amps approx.
- 22 V @ 0.83 amps approx.
- 28 V @ 4.50 amps approx.

66. Antenna azimuth beamwidth: -

Transmit	90°
Receive	49°, each of two

67. Antenna elevation beamwidth: -

Transmit	21.5°
Receive	21.5°

68. Azimuth beam pointing angle: -

Transmit	0°
Receive	$\pm 20^\circ$

69. Elevation beam pointing angle (from antenna axis):

Transmit	-34°
Receive	-34°

70. Antenna peak gain (at pointing angles): -

Transmit	11 db
Receive	14 db

71. Antenna RF bandwidth (- 1/2 db) $\geq$ 9 mc/s

72. Number of rows of elements in antenna 2

73. Total number of antenna elements 2 x 17

1.7 SYSTEM CONFIGURATION

The system will be installed in the vehicle as three assemblies. The electronics will be in the right side equipment box between stations 479 and 565. If the problems created by full wave-length spacing can be resolved, the two antennas will be in the wiring troughs on each side of the vehicle between stations 479 and 720. Interconnections between the right and left side will be made through the wheel well. Since the transmitting antenna and the electronics will require a one inch diameter interconnecting coaxial cable to handle the high power, the transmitting antenna will be on the right side to limit the length of the 1" diameter cable that is required. The left side antenna serving as receive only, with no high power requirement, will require a smaller diameter interconnecting cable.

1.7.1 Antenna

The antenna installation will consist of a rectangular sheet of dielectric material approximately 21 feet long by 11 inches wide. This sheet will replace the trough covers and be made the thickness required to satisfy structural requirements. On the sheet will be a series of "boxes" 7 inches wide x 14 inches long and 2 inches deep. These "boxes" will be spaced on 15 inch centers and when installed will insert between station frames. The 2 inch height of the box will enable it to stay below the top of the station frame members.

The boxes will be connected in series by coax cable through connections at the sides of the box. The duplexer and coax connections to the boxes will be limited to 1 inch in height and increase the overall width of the box to approximately 9 inches. It is anticipated that this

approach will permit the box interconnection cables to go under the frames which are recessed 1.10 inches in the trough area. This will allow the entire assembly and disassembly of each antenna in one piece.

1.7.2 Radar Electronics

The radar electronics will be installed in the box structure supplied by the user along with the RF parts of the right side direction finding (d.f.) antennas and the cooling system. The box will then be installed through a hinged door and hard mounted to the airframe.

The d.f. RF parts and the cooling system will be hard mounted to the inside of the box, however, there will be thermal insulation inserted at each mounting point.

Except for the filter box, the entire active radar will be vibration isolated from the box. In fact, the transmitter-receiver unit will have dual isolation from the box.

The radar electronics will consist of five separate chassis that will assemble through the box cover onto the vibration isolation system using standard military electronic equipment clamps (NAS-573). These fasteners will permit the assembly and disassembly of the radar electronics without the use of tools of any kind.

The five chassis are the power supply, transmitter-receiver, clutter tracker, filter bank and the data processor. A list of the weight volume and power dissipation is shown in Table 1-3.

TABLE 1-3

SYSTEM WEIGHT, VOLUME AND POWER

UNIT	WEIGHT-LBS.	VOLUME FT^3	PWR.DISS.-WATTS
Power Supply	64	1.6	360
Trans-Receiver	89	2.2	2087
Clutter Tracker	18	0.4	55
Filter Bank	10	0.4	45
Data Processor	13	0.5	70
Frame & Interconnections	35	1.3	10
Total	229 Lb.	6.4 Ft.^{3}	2627 Watts

1.7.3 Cooling System

Preliminary analysis of the cooling system indicates that up to seven fans and heat exchanger units will be installed in the upper back triangle portion of the box. As of now it is intended to use the 1 gpm pump, reservoir, filter and heat exchanger units that are presently used in the other system using the box. It is intended that approximately 2400 watts of the 2627 total shown in Table 1-3 will be cooled by the liquid directly. The fan-heat exchanger units will be used to eliminate the remaining power dissipation, environmental and cooling system load.

The OS-25 cooling fluid will enter the rear of the box through a self-sealing connection, pass through the filter and go in parallel through the fan-heat exchanger units. The fluid will then pass through the power supply chassis to cool the high voltage components and the low voltage regulator power transistors. From the power supply the fluid will go to the transmitter-receiver to cool the limiter, power tube and duplexer. From the transmitter-receiver the fluid will be pumped out of the box through another self-sealing connector.

Calculations indicate the fluid will have a 60°F temperature rise in the box and assuming a 95°F inlet temperature will result in a 155°F outlet temperature during radar operation.

1.8 CLUTTER FLIGHT TEST PROGRAM

1.8.1 Purpose

To determine the radar reflectivity of various types of terrain in the 200 mc. region. The terrain to be evaluated includes flat land, two aspects of a city, a bay, forest and mountains.

1.8.2 General Description

In the initial planning, the company's DC-3 was to be utilized for the flight program. As this aircraft was sold before the tests, a Beechcraft of the Queenair type was modified for the flights. These modifications included structural additions to mount a vertically polarized antenna on the right side of the aircraft and to mount the transmitter, receiver, display and recording instruments within the aircraft.

A Navy type SK radar transmitter was used. To physically fit in the aircraft it was cut into two parts and rewired. The Vitro model 1306 receiver was also modified to remove all coupling time constants.

A mock-up of the antenna reflector portion of the aircraft's surface was made to facilitate the measurement of the antenna pattern and gain on the antenna range. The aircraft structure and equipment modifications are completed and the system is in operating condition.

The first data flight has been made with the radar equipment operating satisfactory. This data plus that from additional test flights will be processed to determine a median value of reflection coefficient for each type of terrain. If possible, the results will be compared to results of similar tests run at other frequencies by

the Naval Research Lab (NRL) and Stanford Research Institute. Acknowledgment must be made of the ideas and techniques derived from NRL and SRI project reports and particularly from a visit with Mr. N. W. Guinard of NRL.

1.8.3. Equipment

Beechcraft Queenair aircraft

Navy type SK radar transmitter

Vitro receiver model 1306

Measurements Corporation signal generator model 80

Dummy load - Bird model 82A

Airborne Instruments Lab power oscillator type 651

Termaline wattmeter model 611

Tektronix oscilloscope type 545

Blue band duplexer for type SK radar

Vertically polarized side looking antenna

Camera

1.8.4. Procedures

The procedures used in operating and calibrating the system and measuring and processing the data will be described briefly here in terms of the conduct of a typical flight. The specific procedures may be conveniently divided into three groups: preflight checks on the ground, calibrations and measurements during the flight, and post flight data processing.

During the initial calibration of the system on the ground, the transmitter is tuned to operate on the assigned frequency of 219 mc. and the pulse length and peak radiated power are accurately determined.

For initial calibration, the system is connected as indicated in figure 1.6. The duplexer is terminated with the dummy load and the limiter and switch. The transmitter and duplexer are then tuned to 219 mc.

To calibrate the peak power output and accurately determine the pulse length, the system is connected as indicated in figure 1.7. The duplexer is detuned and utilized as an uncalibrated directional coupler. The type 651 oscillator is set to operate in a CW mode and the oscillator coupling adjusted to give a 10 watt output. The transmitter output is then measured by comparison to the calibrated 10 watt signal through use of the variable attenuator, and the exact pulse duration determined on the detected pulse on the oscilloscope. If possible, the return from a stationary target will be maximized by tuning the duplexer with the antenna connected to the system as shown in figure 1.6. This completes the preflight calibrations and measurements.

In flight, the receiver will be tuned to the transmitter frequency, and the receiver gain will be adjusted so that 95% of the returns fall on the face of the scope. Roughly 240 picture frames of data will be taken for each type of terrain. Immediately after recording the data, the receiver gain will be calibrated at four signal levels provided by a CW signal generator. The calibration will be recorded on film and the signal level out of the signal generator will be logged. This completes the in-flight calibrations and measurements.

Data processing will begin after the flight films have been developed. Individual frames will be projected upon a screen or blank wall for manual measurement. Vertical displacements will be measured

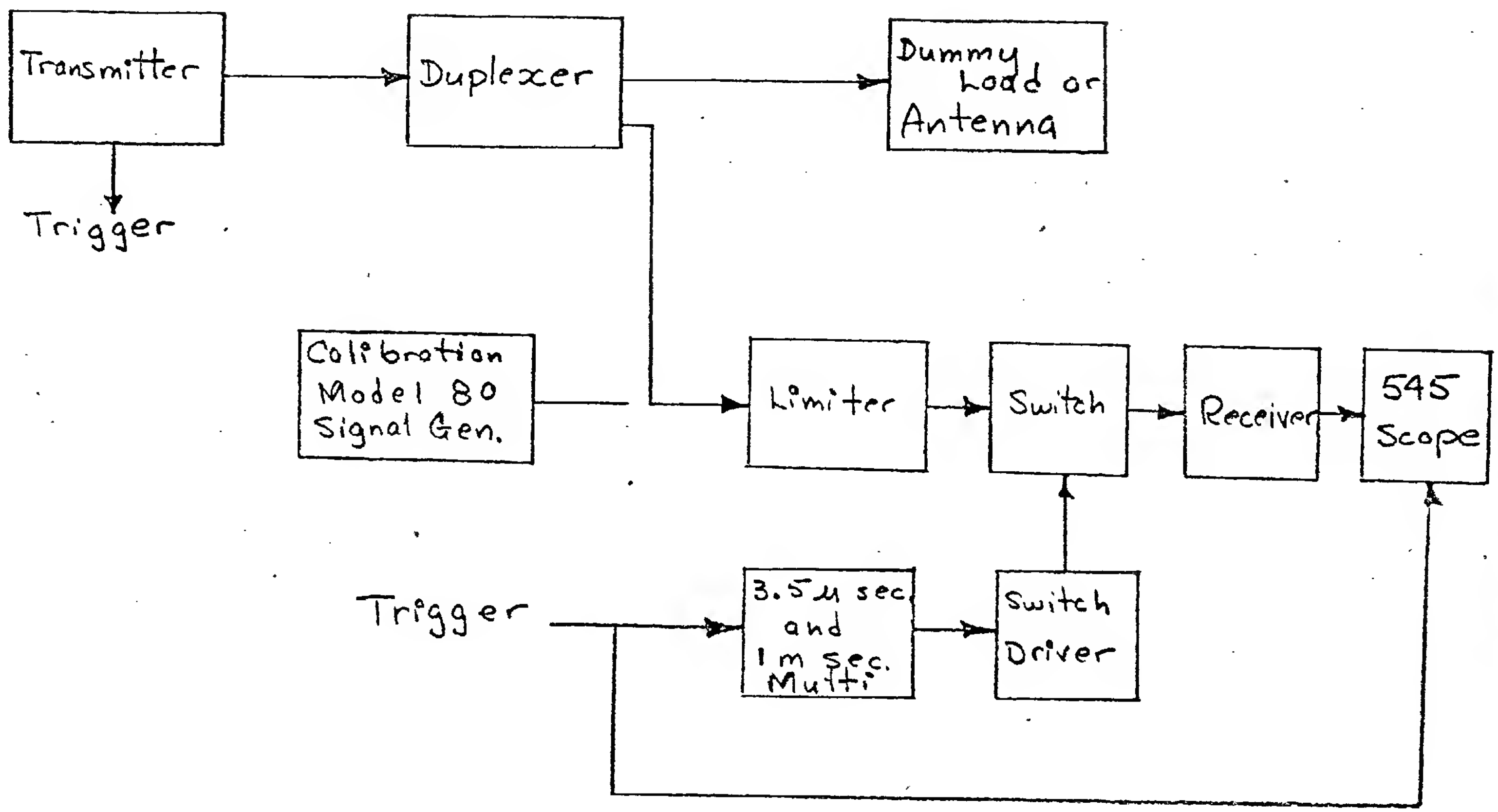

Figure 1-6 Clutter Flight Test System Block Diagram

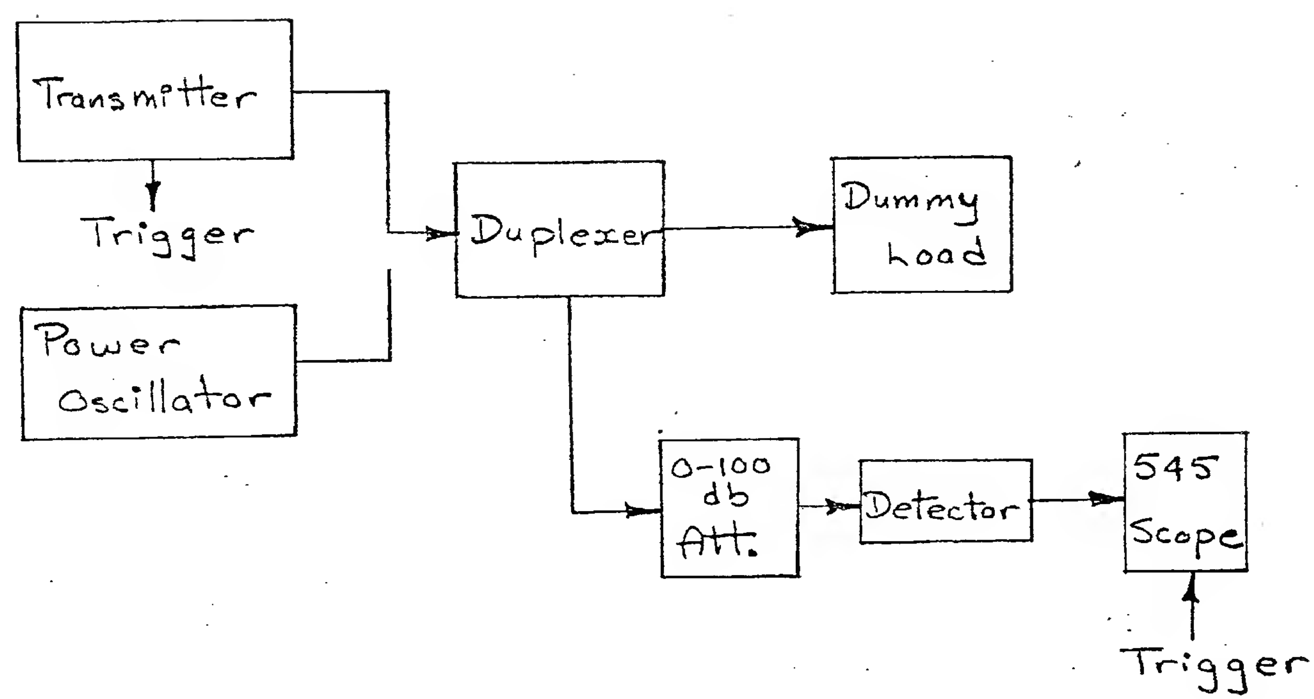

Figure 1-7 System Configuration for Calibration

at horizontal displacements corresponding to time delays calculated to correspond to selected slant ranges which in turn correspond to the desired downlook angles. The calibration data will then be used to convert the measured displacements in distance units to voltages. The median voltage return for each downlook angle will be determined for each run. The expected downlook angular coverage is roughly 10^{o} to 60^{o}. The median value is used instead of the average at the suggestion of NRL. Finally, the median voltage returns will be used to compute $_{o}$, the radar area per unit of horizontal area of terrain, according to the NRL formula

$$_{o} \quad P_R(4\pi)^3\, R^4/P_T\, G^2 \quad {}^2\, A$$

where P_R received power

R mean range to target area

P_T transmitted (peak) power

G antenna gain

wavelength

A approximate horizontal area from which all observed contributions to the echo came. P_R will be calculated directly from the median voltage return. R will be obtained directly from the time delay of the return. P_T and will be measured directly in the preflight calibrations. G has been measured using the radar antenna and a mock-up of the aircraft on an antenna range. In calculating A, an equivalent rectangular beam pattern will be used having a uniform two way power pattern equal in azimuth to the measured two way 3 db beam pattern and determined in elevation by the transmitted pulse width.

2. ACTIVE SUBSYSTEM MECHANIZATION AND INTEGRATION

2.1 MECHANIZATION AND SEQUENCE OF OPERATION

The design of the active radar system is progressing along the lines originally set forth in the proposal. Briefly, the principles employed are as follows:

A stable RF frequency is transmitted from one antenna which covers the terrain of interest ahead of the vehicle ground clutter and returns from fixed velocity and accelerating targets are received on two antennas, relative signal strength being a function of their coverage on each side of the vehicle. Two receiving channels are used, one for left and one for right coverage. All returns not doppler shifted by a velocity greater than the vehicle velocity will appear in the receiver as part of the clutter return. On each receiver there is a fixed frequency single side clutter reject filter which will attenuate this clutter about -30 db.

Two techniques are available to keep the clutter positioned in this filter. First there is available the vehicle velocity, therefore, the transmitted frequency may be adjusted in direct proportions to this velocity to insure the unwanted doppler return falling within the reject band of the clutter filter. Although this is an open-loop technique it is the one most often employed, and has received most of the design attention to date.

In addition, clutter may be close-loop tracked by periodically shifting some of the clutter beyond the filter reject region to develop enough error voltage to permit close edge tracking of the clutter reject skirt.

This second technique will receive more design attention in the coming months.

Any radar echo received which has a velocity component toward the approaching vehicle will be doppler shifted in excess of the clutter doppler and therefore will continue past the clutter reject filter to the filter bank. Both fixed velocity and accelerating targets are detected. However, only targets accelerating a critical amount will advance through the filter bank causing a second detection in filters displaced $3\frac{1}{2}$ to $7\frac{1}{2}$ filter widths higher in frequency then their location on the first detection. The entire data processing hardware is devoted to determining this critical displacement for alternate "looks" and causing a display of right or left alarm zone; concurrent with processing all data to reject all other radar echos not so shifted in doppler frequency.

2.1.1 Present System Mechanization

To better illustrate the areas of change between the proposed and present block diagrams, both are shown in Figures 2.1 and 2.2. In the current block diagram note the following areas of change:

(a) Clutter rejection requires that the clutter doppler frequency be mixed with a variable frequency to position the clutter in the fixed frequency filter. This tracking may be achieved by varying the LO frequency, as proposed, or the RF as previously described for the current design. Either technique is satisfactory.

(b) The clutter track loop is closed after the third IF (tracking the edge of the clutter filter) instead of through one of the filters in the filter bank because the sawtoothing reduces the duty cycle of the error voltage present in the filter bank, where as the clutter frequency

SPECIAL HANDLING

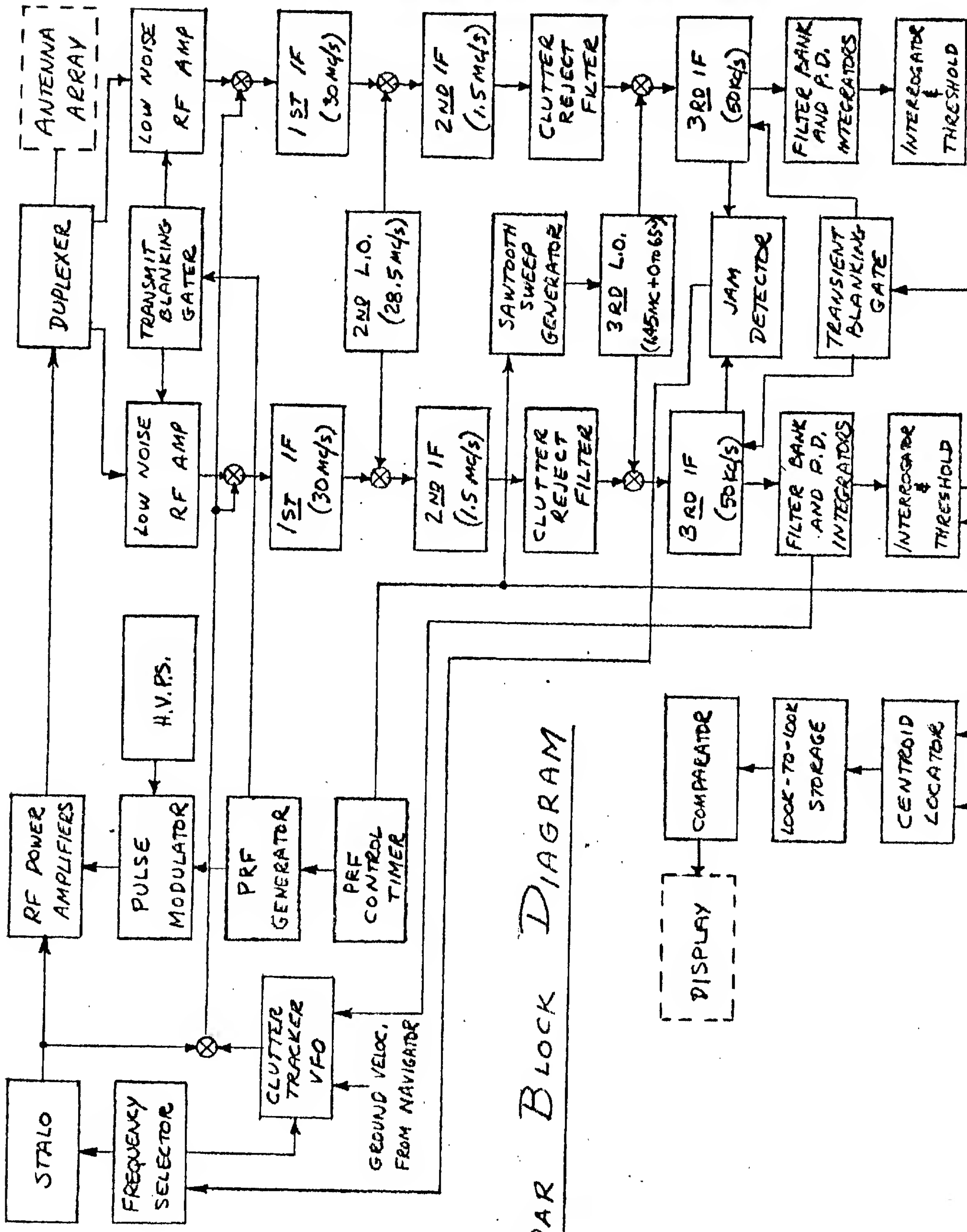

RADAR BLOCK DIAGRAM

Figure 2-1 Radar Block Diagram (Obsolete)

SPECIAL HANDLING

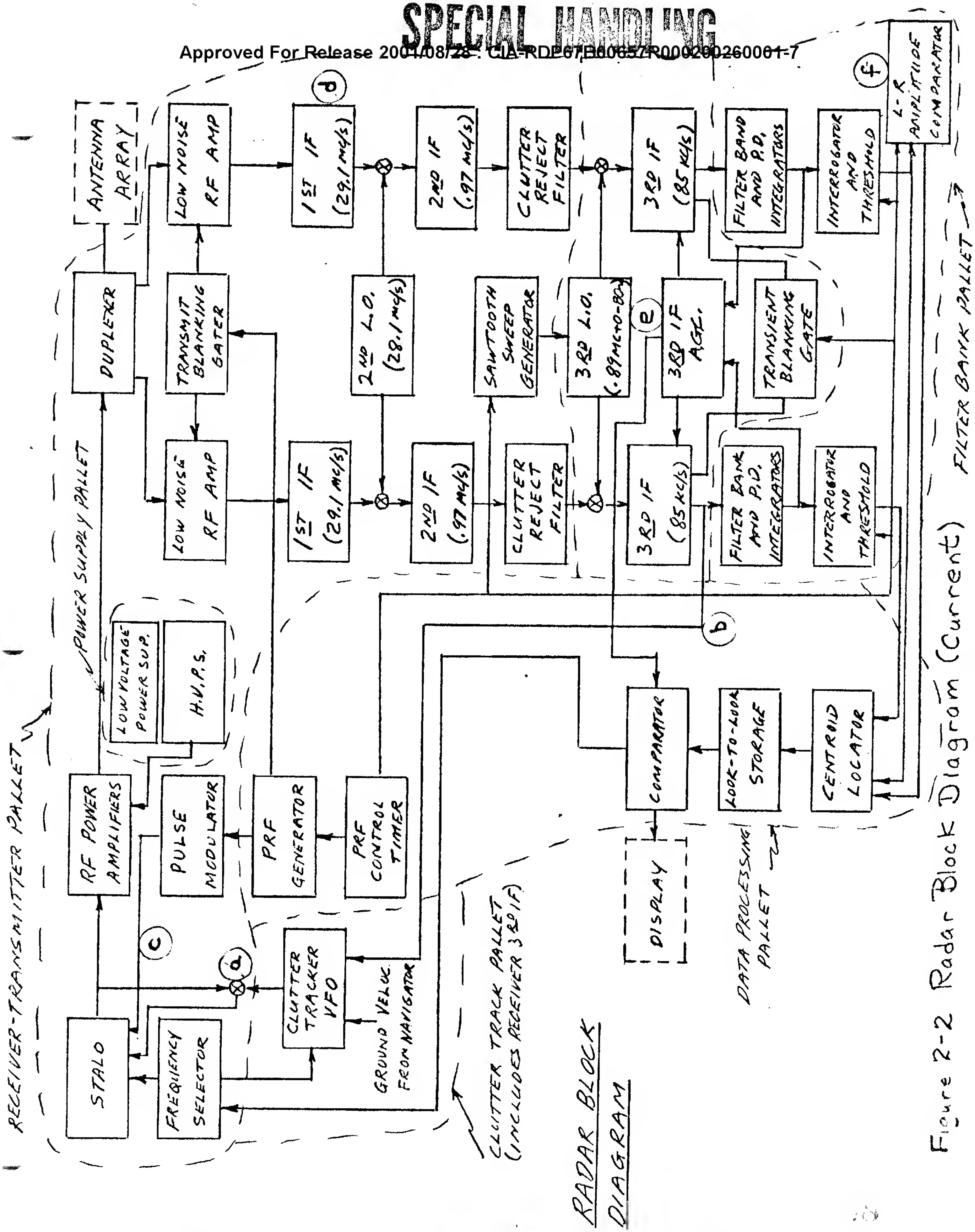

Figure 2-2 Radar Block Diagram (Current)

is undisturbed at the reject filter.

(c) The transmitter on-off time is determined by gating the stalo instead of the RF amplifier, thereby eleminating high voltage, high power, grid modulation in the final amplifier.

(d) The IF frequencies were changed to keep PRF harmonics out of the passband.

(e) The level of jamming interference is determined by monitoring the third IF AGC which in turn is used to control the system frequency diversity operation as discussed in a following paragraph.

(f) An amplitude comparison circuit has been added to prevent two channel alarms for large signals in the following manner.

The data processor scans each filter bank to determine a left or right azimuth target. If the target echo were large enough to be detected in both channels the proposed data processor would have made no choice between left or right alarm. Therefore, the filter bank scanning has been re-designed to inhibit the alarm from the weaker channel. Figure 2.3 accompanies the following description of this circuit.

Each filter in the bank is non-destructively scanned twice during the detector-integrator read out time. During the first scan of all 40 filters the L>R gate is present and each filter in the left bank is compared in amplitude with the corresponding filter in the right. This filter-by-filter comparison results in a signal output pulse only if the left bank amplitude exceeds the right. Both banks are scanned simultaneously a second time only now a signal output pulse is sent to the centroid locator only if right bank amplitude exceeds left.

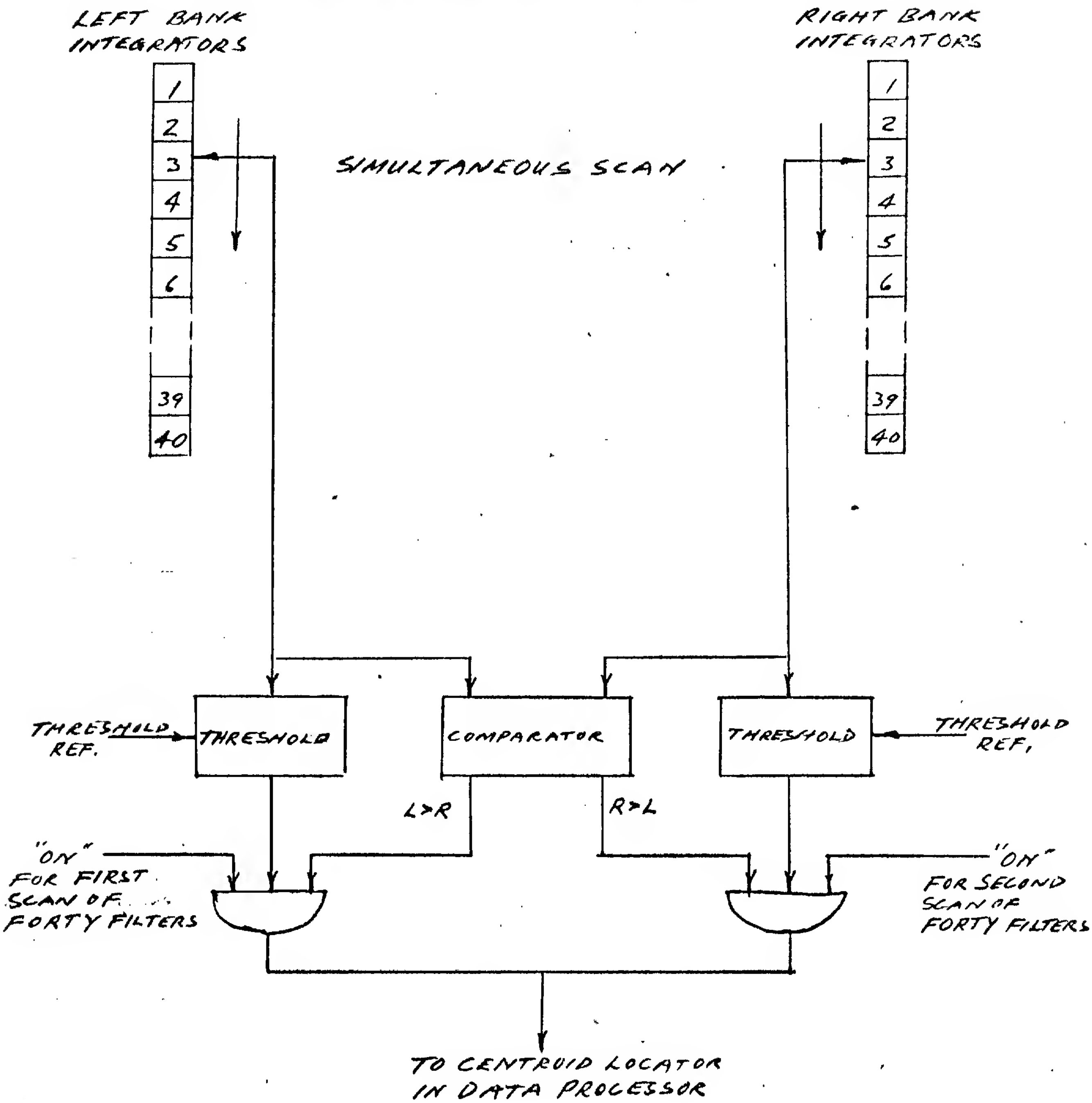

Figure 2-3 LEFT-RIGHT AMPLITUDE COMPARATOR

2.1.2 Frequency Diversity and Jam Avoidance

Before beginning a discussion of the system timing and sequence of operation it may be well to point out one area where present design does depart from the proposal.

The proposal states, "When jam or interference is detected a search for a clear channel is made by the selector. If no clear one is found the selector has memory which picks the frequency which gave the lowest level of interference. Subsequently, a new search is made periodically say once a minute, until a clear channel is found". The following technique is now believed to be superior, and has been included in the present design.

Seven transmit frequencies, each shifted about one megacycle, are available. The system will transmit on one frequency and PRF for one filter bank integration time, then move to the next frequency and PRF for the next integration time. It will continue to switch between two PRF's as it alternately samples each available RF frequency. When the clearest channel is located the system will remain at that frequency but will alternately continue searching for a clear channel. Note that when a "hit" (radar echo detected in the filter bank) occurs the system holds the same RF and PRF for the next look period. Figures 2.4 and 2.5 illustrate this sequence. Only five frequencies are shown instead of seven; and the events are explained in greater detail in the following paragraph.

2.1.3 Sequence of Operation

The previous section with Figures 2.4 and 2.5 has explained the sequence of operation as a function of jam and target detection. This section will provide additional detail. Figure 2.6 will be needed to follow each step.

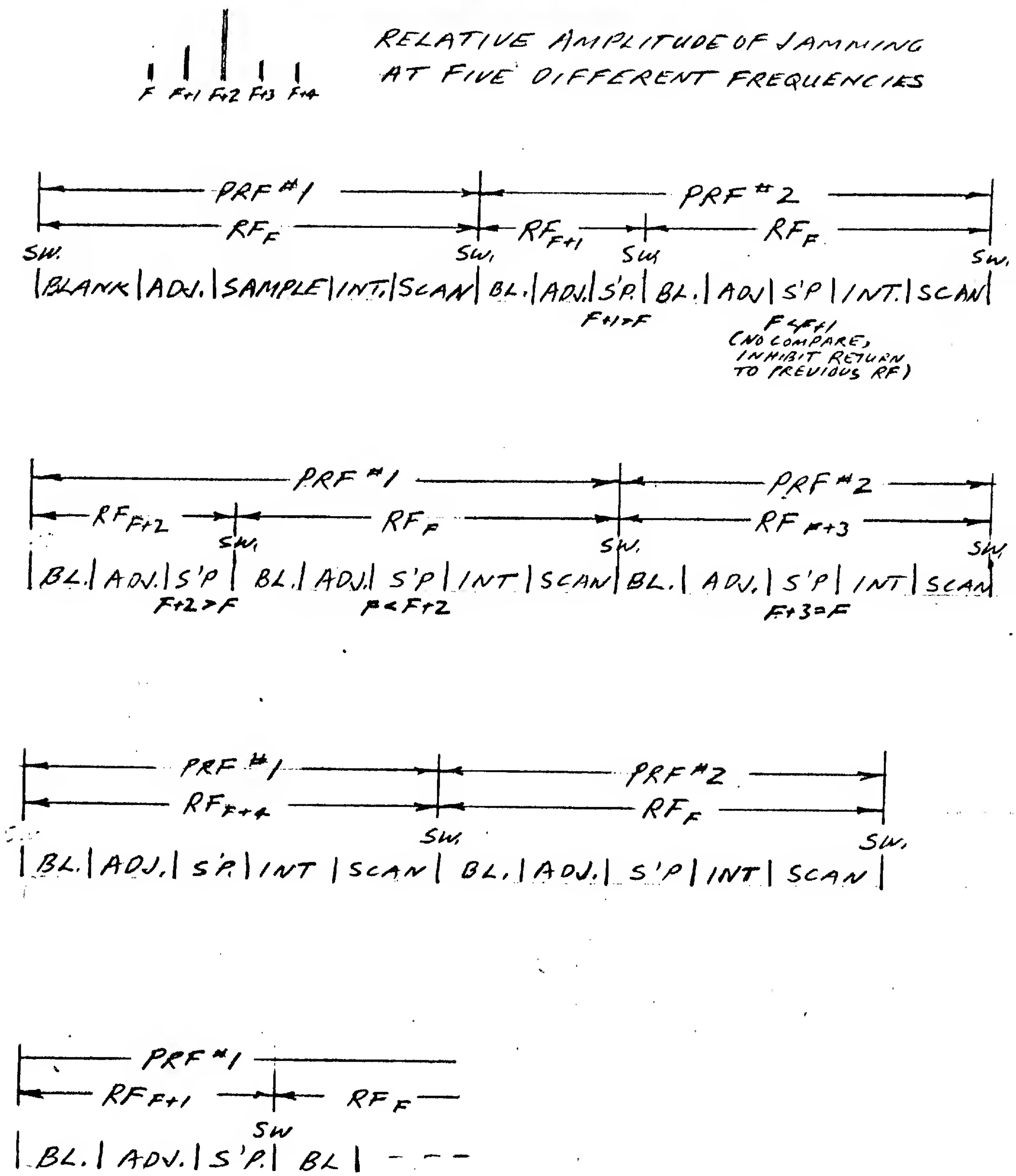

Figure 2-4 SEQUENCE OF OPERATIONS IN A JAMMED ENVIRONMENT ([illegible])

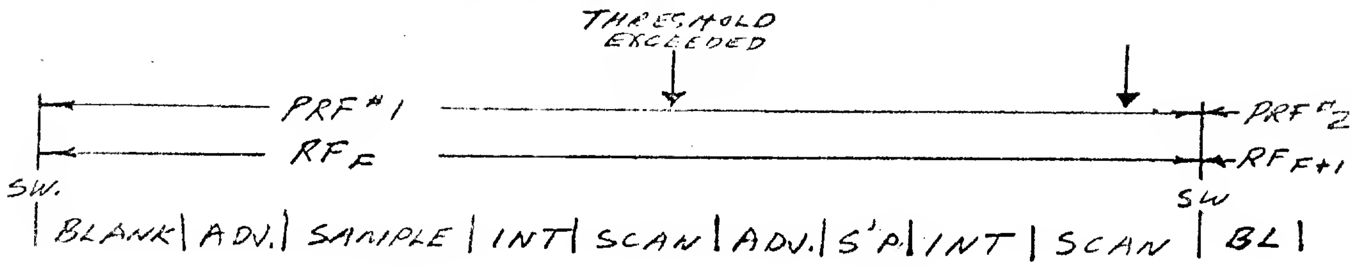

Figure 2-5

SEQUENCE OF OPERATIONS
FOR ONE HIT OR TWO HITS

JAMMING ON SAMPLED FREQUENCY POORER THEN PRESENT FREQUENCY

INTEGRATE	READ OUT NO HIT OR SECOND HIT	SETTLE TRANSIENT BLANK	AGC ADJ.	SAMPLE	COMPARE	SETTLE	AGC ADJ.	SAMPLE	INTEGRATE
290 MS	1.88 M.S.	50 MILLI S.	50 MILLIS	≈ 10 μs	≈ 6 μs	50 M.S	50 M.S.	10 μs	290 MILLI
	SW RF-PRF				SW RF				

CLAMP INTEGRATORS

JAMMING ON SAMPLED FREQUENCY BETTER THEN PRESENT FREQUENCY

INTEGRATE	READ OUT NO HIT OR SECOND HIT	SETTLE TRANSIENT BLANK	AGC ADJ.	SAMPLE	COMPARE	INTEGRATE
290 MS.	1.88 MS.	50 M. S.	50 M.S.	≈ 10 μs	≈ 6 μs	290 M.S.
	SW RF-PRF					

CLAMP INTEGRATORS

FIRST HIT (FOLLOWING INGEGRATION PERIOD FOR ABOVE "NO HIT")

INTEGRATE	READ OUT FILTER BANK FIRST HIT	AGC ADJ	SAMPLE	INTEGRATE
290 M.S.	1.88 M.S.	50 M.S.	≈ 13 μs	290 M.S.

Clamp Integrators

SEQUENCE OF OPERATIONS TIMING DIAGRAM

Figure 2-6

Two hundred and ninety milliseconds are provided for the radar echo to be separated in the filter bank, detected and integrated. After this the filter bank is scanned. If no bit occurs the RF and PRF are switched and 50 milliseconds are permitted for system transients to settle before the AGC adjust period begins.

If one detector-integrator has a charge above the threshold level a "bit" is recorded inhibiting RF and PRF switching. After the AGC voltage has adjusted the data processor samples its present value to compare it (using 12 step quantization) with the AGC value in the next period.

2.2 TRANSMITTER AND R.F. CIRCUITS

The transmitter specifications and configurations have changed to meet system specifications and to reduce size and weight. The original and present general specifications are listed below:

Table 2-1

Transmitter Parameters

	Original	Present
f_o	200 mc	242.1 mc
f_{bw}	20 mc $\pm$ 3 db	10 mc $\pm$ 2 db
P_{avg}	1 kw	2 kw
P_{peak}	2 kw	$\approx$ 4.2 kw
duty cycle	0.5	$\approx$ 0.48
sidebands	85 db below carrier at 100 cps	

Figure 2-7 shows a block diagram of the present transmitter configuration. It is planned to place all of these units on a doubly mechanical isolated platform because many of the units will marginally meet the spurious sideband requirements if subjected to the fundamental structure vibrations.

The fundamentally difficult areas were investigated first. These are:

1. 30 mc crystal oscillator (vibration)
2. Transmitter basic oscillator (vibration)
3 Transmitter solid state amplifier (overall design)
4. Final amolifier (overall design & vibration)
5. Duplexer (high average power & signal purity)

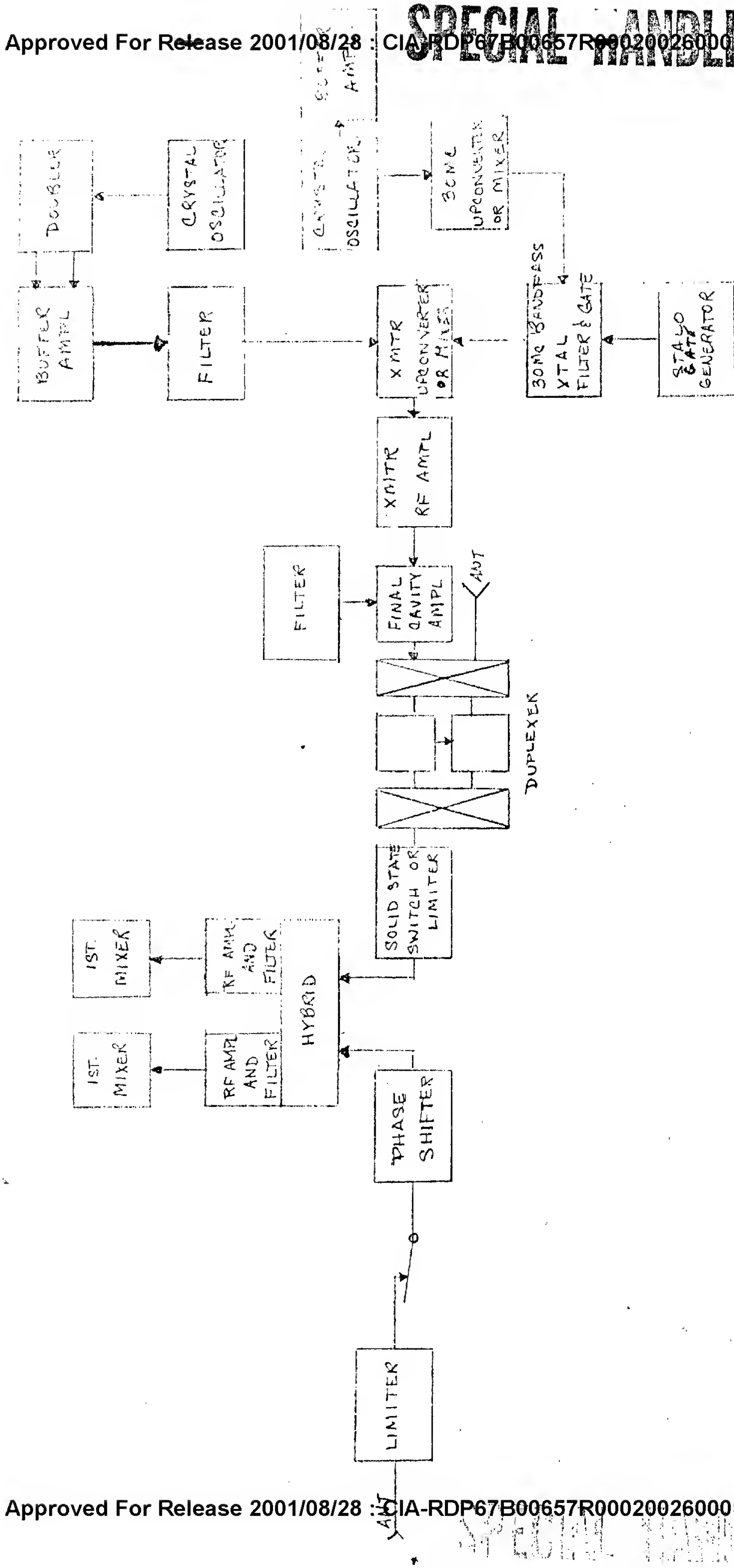

Figure 2-7 Transmitter Block Diagram

SPECIAL HANDLING

6. High power limiter

7. High voltage power supply

Items 1, 2 and 3 being solid state, these units were under taken by personnel skilled in solid state techniques. A general review of the specifications and their relationship to previously known techniques was under taken as a study effort.

Items 4, 5 and 6 were reviewed and tentative specifications written.

Item 7 was reviewed with the possibility of reducing weight and size.

Other units on the block diagram were reviewed and found to be off the shelf items with only a few modifications necessary.

2.2.1 <u>Crystal Oscillator Stability</u> (Items 1 & 2)

The question of short-term stability, in the form of FM sidebands, is of prime importance in this project. The initial requirement is that FM sidebands should be 85 db down at a vibration frequency of 100 cps or greater.

The oscillators selected are of the Pierce type, using 2N918 transistors in the grounded-emitter configuration with feedback taken from the collector to the base.

It has been shown that all fundamental types of oscillators have the same stability, and that this stability depends primarily on the Q of the resonator and on its physical stability. The resonator used in this case are quartz AT-cut crystals, packaged in ruggedized cans. Two

crystal packages were evaluated, both developed by Bell Telephone Laboratories for satellite use.[1]

The test arrangement used to measure the FM sidebands is shown on figure 2-8. Two oscillators of identical design are fed into a diode mixer and the output fed to an amplifier with a 1 mc cut-off frequency, thereby eliminating the high-frequency mixing products. The 180 kc difference-frequency signal goes into the second i.f. input of the LFE Stalo Tester, and its output is inspected in 7-cycle strips by the HP 302 wave analyzer. The output of the Stalo Tester had been previously calibrated for conversion of volts to FM deviation. The FM sidebands are then given by the formula:

$$(\text{sideband in db}) = 20 \log_{10} \frac{\Delta f}{2 f_o}$$

where: Δf = FM deviation as measured on wave analyzer

f_o = frequency of disturbance (vibration or ripple)

NOTE: In the case of the noise level Δf was multiplied by .707 assuming the equi-partition of noise.

The oscillators were subjected to two kinds of stresses; vibration and voltage supply variation. In the case of vibration, the crystal packages by themselves were cemented down to a small Calidyne shaker (2 1/2" diameter) and connected by short leads to the rest of the oscillator strapped to the bench above it. In the case of the crystal packaged in a TO-5 Header from Monitor Products, no FM sidebands were found even

1. W. J. Spencer and W. L. Smith, "Precision Quartz Crystal Controlled Oscillator for Severe Environmental Conditions", Proceedings of the 16th Annual Symposium on Frequency Control. pp 405-421, April 1962.

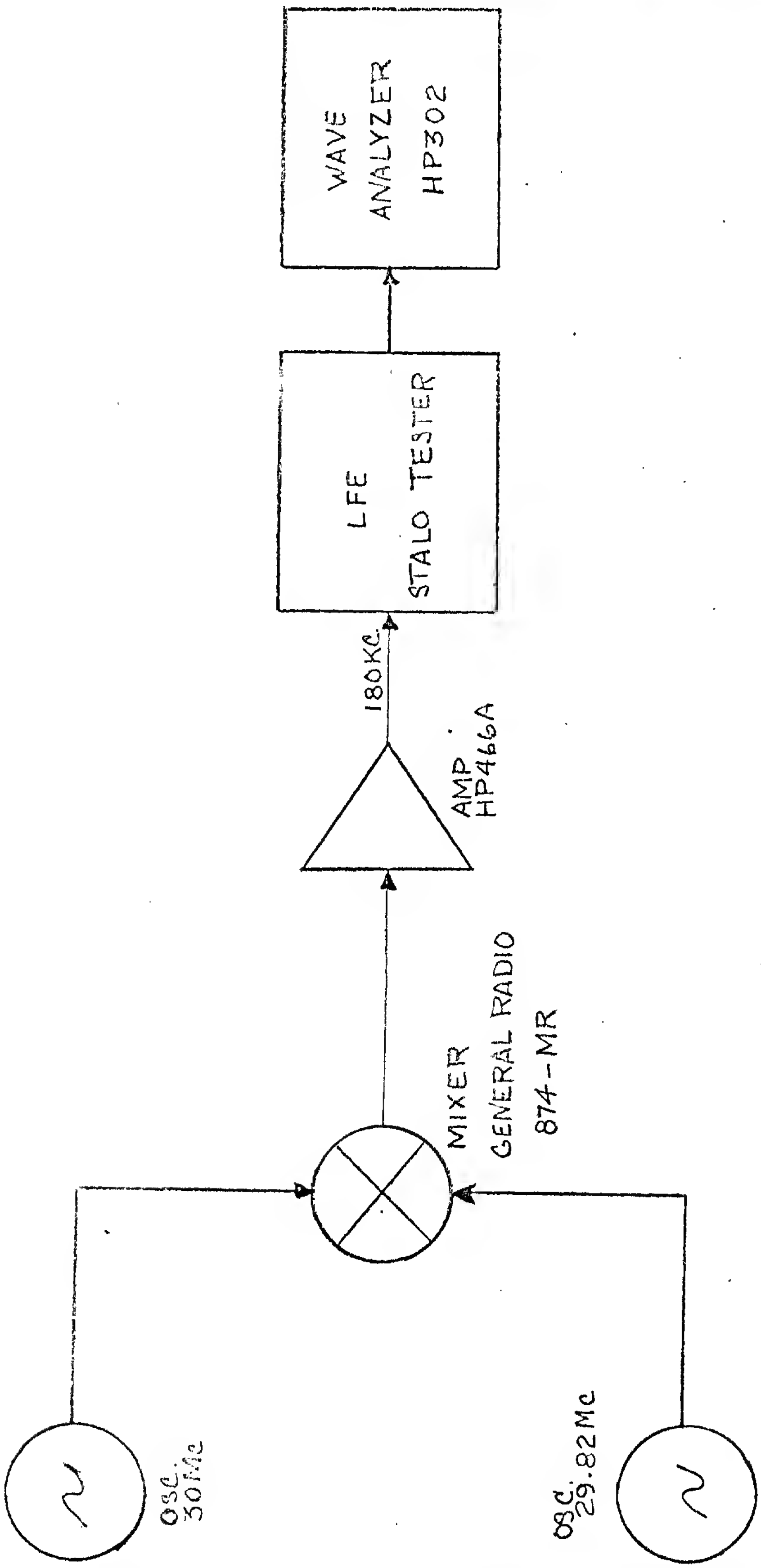

Figure 2-8 TEST ARRANGEMENT FOR MEASUREMENT OF FM SIDEBANDS

though it was vibrated at levels as high as 10 g's in the range from 100 cps to 2 kc, (i.e, any sidebands that might arise were limited by the noise level of the measuring system. On the other hand, a simple interchange of crystals showed that sidebands could be easily obtained from the physically larger Bliley crystal at 1 and 2 g's. Thus apparently if the small crystal in the TO-5 can is used, packaging problems will be considerably reduced. Results of the vibration tests are shown on figure 2-9.

To introduce ripple into the voltage supply of the oscillator, a filament transformer was inserted in the line and a low frequency sine wave generator connected to the opposite winding. The results for this test are shown on figure 2-10. The ripple amplitudes at which FM sidebands become undistinguishable from noise level have been indicated at several points on the noise-level curve.

2.2.2 Solid State Power Amplifier (Item 3)

In the initial design phase of the transmitter attempts were made to purchase a solid-state power amplifier capable of supplying 8 to 10 watts of RF output power in the frequency range of interest. However, due to the security requirements of the contract, it was not possible to obtain such a unit from the existing supplier. A study was initiated into the design and construction of such an amplifier at Westinghouse. Solid-State high power VHF-UHF amplifier design has been investigated at the Surface Division in connection with a communications transmitter study contract. Discussions with

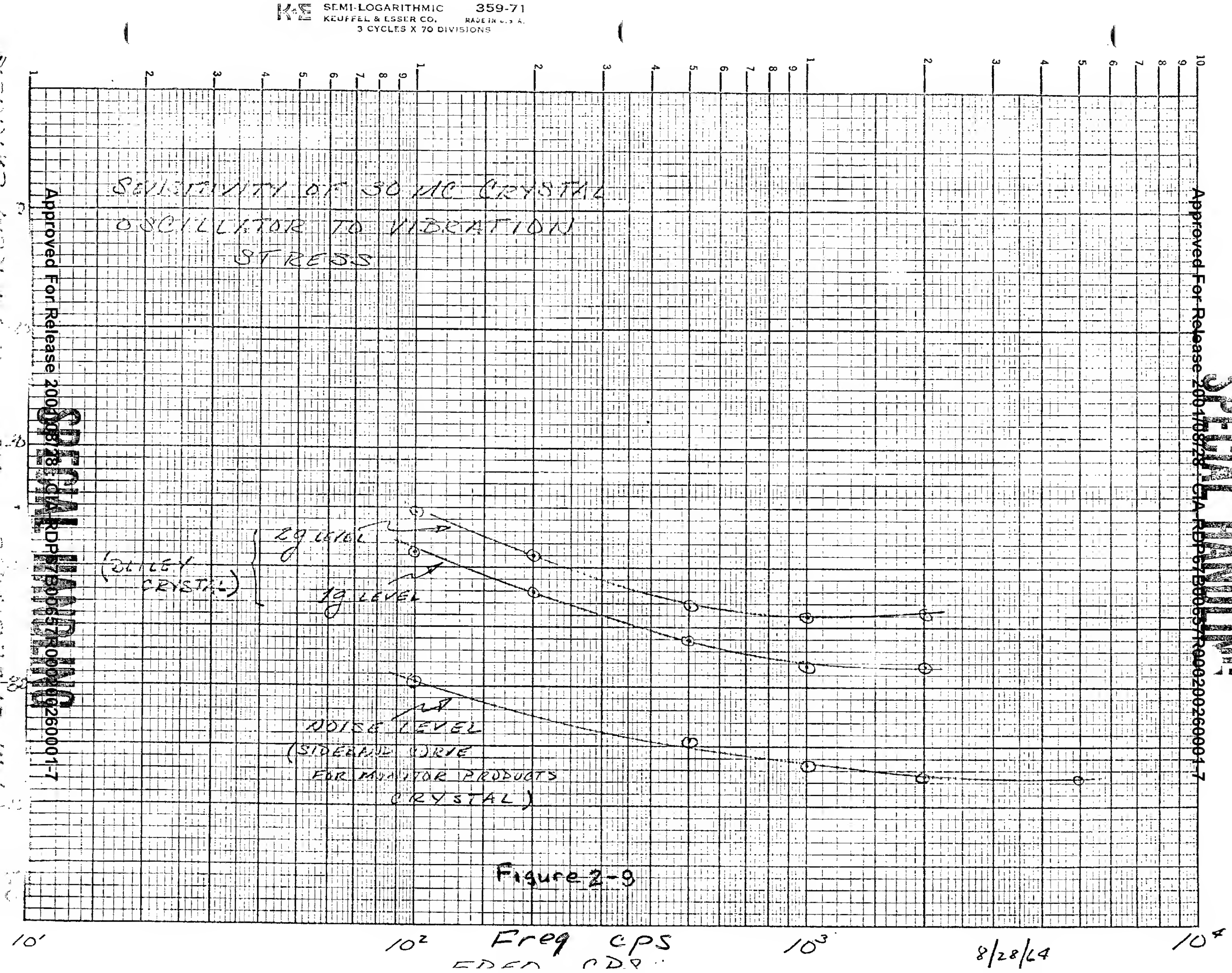

Figure 2-9

SPECIAL HANDLING
Approved For Release 2001/08/28 : CIA-RDP67B00657R000200260001-7

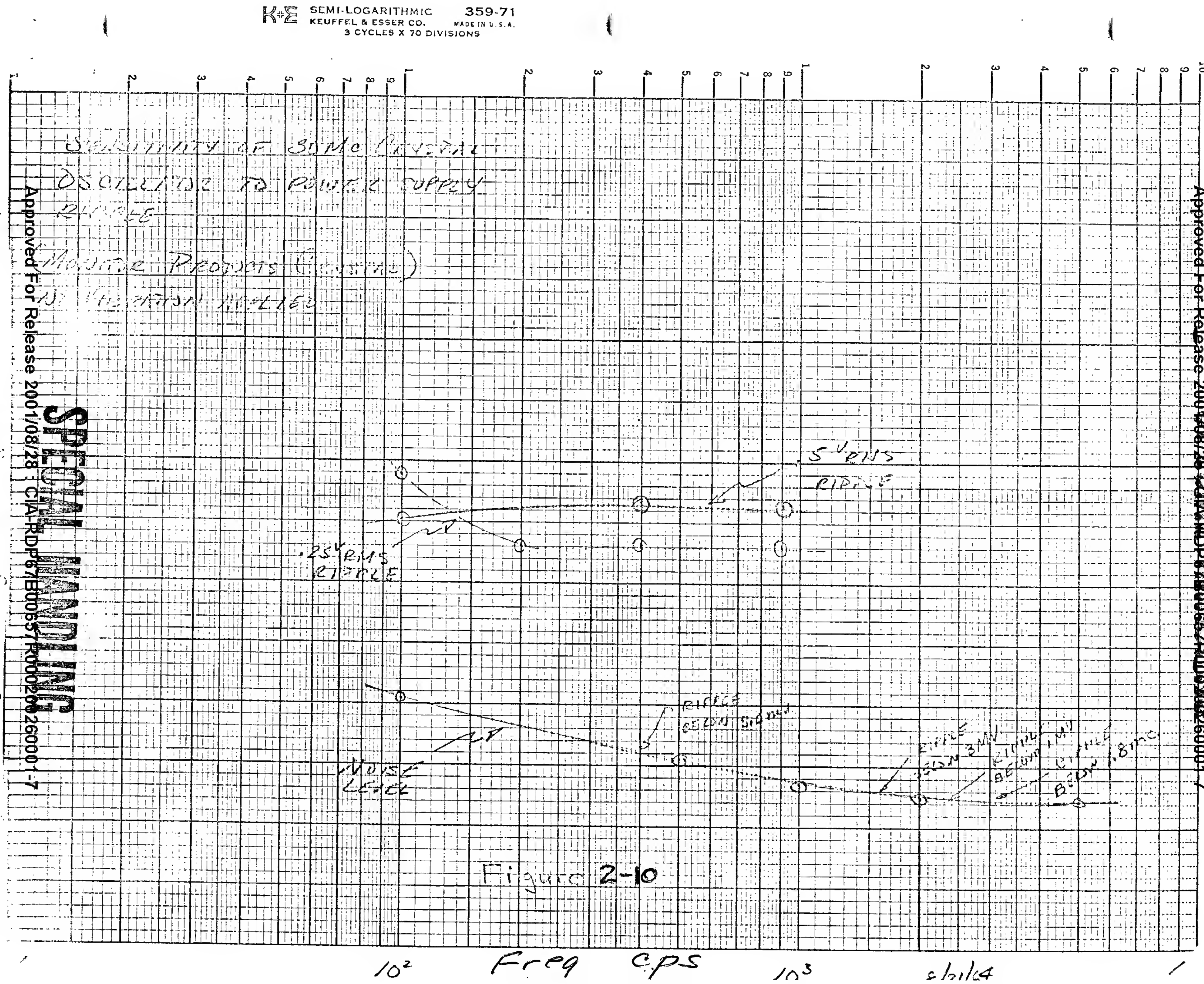

Figure 2-10

SPECIAL HANDLING
Approved For Release 2001/08/28 : CIA-RDP67B00657R000200260001-7

the Surface Division have indicated that it is possible to obtain as much as 35 watts of RF power in a 15% bandwidth by combining the outputs of eight transistors. The transistor used was the RCA 2N3375 which has a maximum dissipation of 11.6 watts at T_c=25°C and is capable of producing a minimum of 3 watts RF output power at 400 mc with a minimum of 3 db of gain. An amplifier with a minimum of 8 watts RF output will be constructed using the 2N3375 transistor. This unit is shown in figure 2-11. It consists of 4 2N3375 transistors capable of dissipating 7.9 watts at a case temperature of 80°C. The driver amplifier will have a gain of 7 db and produce an output of 2.5 watts which will be split equally between 3 power amplifiers. The splitting and summing networks will have an insertion loss of 0.5 db so that the final output will be a minimum of 8 watts.

In addition a study in the areas of efficiency and size is being made as to the possible use of a ceramic tube instead of the solid-state amplifier. This study will determine the configuration of the power amplifier.

2.2.3 Final RF Amplifier (Item 4)

A tentative specification was written and submitted to eighteen (18) possible vendors. As of August 28 fifteen (15) have decided not to respond for various reasons. Two vendors have responded with possible solutions but additional study and effort will be under taken to solve the problem. Those companies which have submitted will be visited in an attempt to evaluate their ability to perform the task.

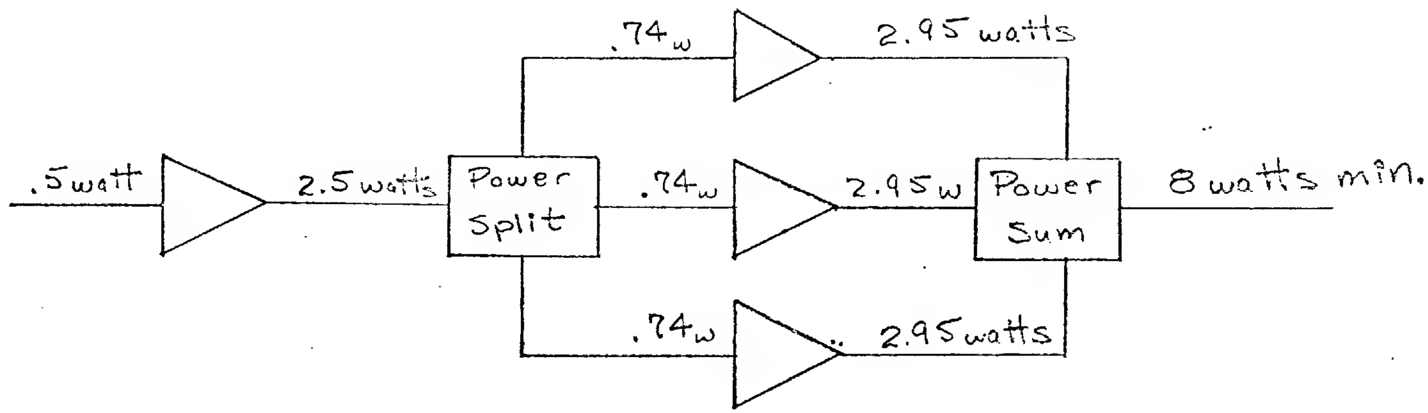

Figure 2-11 Solid-State Power Amplifier

The final power amplifier will consist of two amplifier stages within one package thus minimizing the interconnecting hardware i.e. cooling, R.f. cables, etc. An analysis of vibration effects on coaxial cavities is calculated in section 2.2.3.1. These calculations would indicate that the problems introduced by the vibration level are surmountable.

The final R.f amplifier is a difficult task only when the stability and power is designed into a unit of minimum size and weight with maximum efficiency.

Work will be initiated to determine the exact values of allowable power supply ripple to maintain the spectrum purity.

2.2.3.1 Tuned-Line Deformation

In addition to the FM sidebands that can be generated at the STALO carrier oscillator, sidebands could be generated anywhere else in the system where reactances are subject to one form of modulation or another. It was felt that the tuned-line cavities to be used in conjunction with the output tetrodes could be a potential source of trouble, and therefor the following investigation was attempted.

Three different types of line deformations were investigated: eccentricity, oblateness, and elongation. The FM sidebands arising from an oblate deformation (by which the cylindrical conductors are squashed to an elliptical cross-section) were found to be much smaller than those induced by eccentricity and elongation of the tuned line, and hence will not be treated here.

The formulas used in the treatment of the eccentric deformation were obtained from a solution of Laplace's equation in bicylindrical coordinates.[1]

After a lenghty and involved derivation, we find that the following formulas apply:

$$\frac{1}{C}\,\frac{dC}{ds} = \frac{2S}{(r_2^2 - r_1^2)\ln r_2/r_1}$$

and

$$\frac{1}{L}\,\frac{dL}{ds} = \frac{1}{\ln r_2/r_1}$$

Where S is the center to center displacement of the two conductors and r_1, the outside radius of the inner conductor and r_2 the inside radius of the outer conductor.

Before continuing on the subject of deformations, a small digression will be made so that some of the results can be used later.

To study the amplitude of the sidebands arising from small deformations, a simplified representation of the output of a UHF coaxial tube was used.

In short, we find that the FM sidebands have an amplitude of

$$\text{SIDEBAND} = \frac{|B|}{2G}$$

$|B|$ is the maximum amplitude variation
G is the conductance

relative to the carrier.

B in our case is composed of the output capacitive susceptance of the tetrode together with the inductive susceptance introduced by the tuned line to cancel tube capacitance.

1. See P. Moon and D. E. Spencer, "Field Theory for Engineers" D. Van Nostrand Co. Inc., Princeton, New Jersey 1961.

As an example, we shall consider an eccentric deformation. If $\beta x < 1.3$ radians, then $\frac{2\beta x}{\sin 2\beta x} < 6$, and after several substitutions we find that

$$\Delta B \approx \frac{1}{Z_{in}} \left[\frac{3.5 \Delta s}{\ln r_2/r_1} + \frac{5(\Delta s)^2}{(r_2^2 - r_1^2)\ln r_2/r_1} \right]$$

The results for eccentric deformation are plotted in figure 2-12.

To investigate line elongation, by using

$$\frac{dB}{dx} = \frac{1}{Z_{in}^2} \frac{\partial Z_{in}}{\partial x}$$

since

$$|Z_{in}| = Z_o \tan \beta x \qquad \frac{\partial |Z_{in}|}{\partial x} = Z_o \beta \sec^2 \beta x$$

Therefore,

$$\frac{dB}{dx} = \frac{\beta}{Z_o \sin^2 \beta x}$$

Using this formula, the sideband amplitudes were computed and plotted on figure 2-13 for several values of the parameter βx. Notice that in this graph $G = 10^{-3}$ MHO. If G were let equal to 10^{-4} MHO, the sidelobes would be 20 db higher.

2.2.4 Duplexer (Item 5)

Duplexers of this power level have been built with solid state switches but not specifically at this frequency. It is most desirable to use solid state switches because of their reliability, low weight and small transmission losses.

A tentative specification was written on the duplexer and submitted to eight probable vendors. Of these, four submitted proposals to Westinghouse with detailed drawings. Additional evaluation will be made of each vendor and a final detailed specification written in cooperation with the selected vendor.

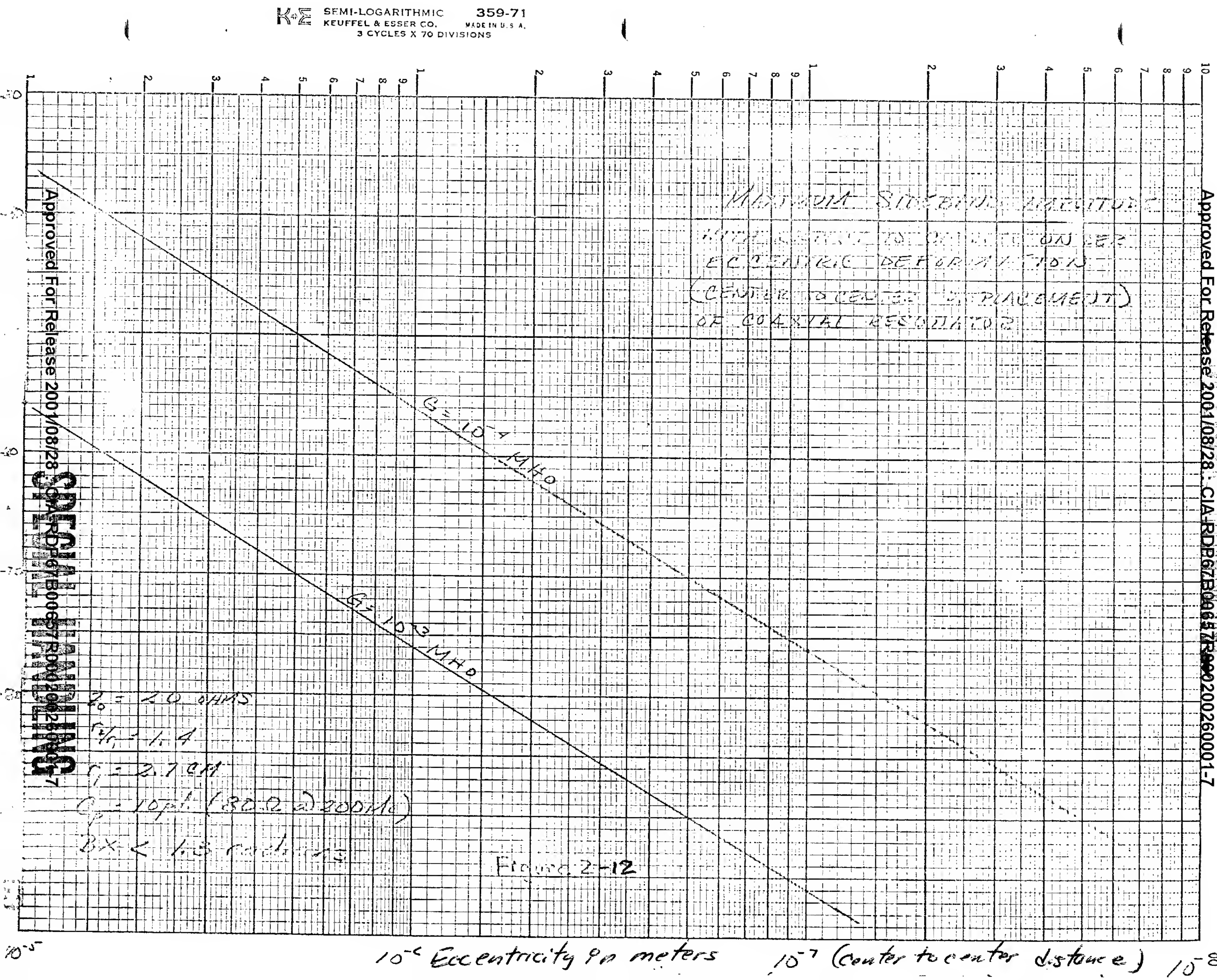
K+E SEMI-LOGARITHMIC 359-71
KEUFFEL & ESSER CO. MADE IN U.S.A.
3 CYCLES X 70 DIVISIONS
MAXIMUM SIDEBAND AMPLITUDE
ECCENTRIC DEFORMATION
(CENTER TO CENTER DISPLACEMENT)
OF COAXIAL RESONATOR
G = 10^-4 MHO
G = 10^-3 MHO
Z0 = 20 OHMS
r2/r1 = 1.4
r1 = 2.7 CM
10^-5
10^-6 Eccentricity in meters
10^-7 (center to center distance)
10^-8

Figure 2-12

SPECIAL HANDLING

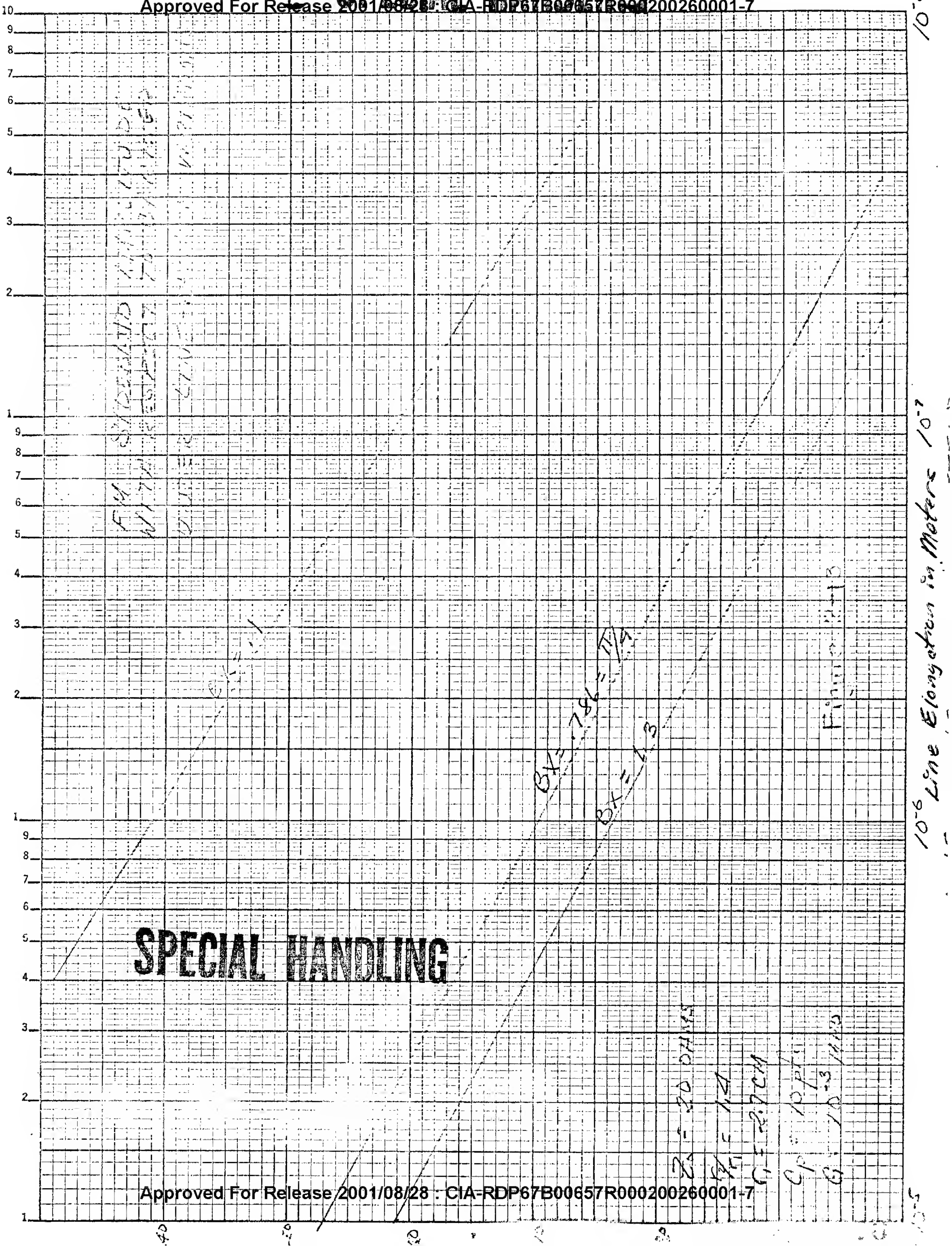

SEMI-LOGARITHMIC 359-71
KEUFFEL & ESSER CO. MADE IN U.S.A.
3 CYCLES X 70 DIVISIONS

SPECIAL HANDLING

The duplexer will have less than 0.15 db loss in the transmit mode. This would indicate a relative low power loss thus eliminating heat sinks, liquid and/or air cooling and the many inherent related complications. Also the duplexer will be self-gated, eliminating the need for a video modulator.

An additional low level gated switch will be inserted between the duplexer and the receiver to provide the required isolation to limit the peak R.f. level at the receiver to 0.2 milliwatts. This unit is off the shelf except for compatible connectors. The above limiter may be incorporated directly into the duplexer configuration to eliminate the losses in interconnecting cables.

2.2.5 <u>High Power Limiter</u> (Item 6)

Because of the proximity of the receive and transmit antennas some 200 watts average will appear in the receive antenna during the transmitter "on" interval. A high power limiter and/or switch will be inserted in the receive arm.

This limiter will be self gating and require no coolant. The energy will be reflected out the receiver antenna and will cause the receive antenna to appear as a secondary transmit antenna. The patterns in the antennas may require additional study but this solution would reduce the problem of removing some 250 watts of heat from the limiter. The limited output value will be 20 milliwatt. Therefore an additional low level gated switch will be incorporated to reduce the level at the receiver terminals to 0.2 milliwatts.

2.2.6 High Voltage Power Supplies (Item 7)

A conventional three phase full wave power supply may be used but all of the latest techniques will be used to reduce weight.

This unit may weigh thirty five (35) pounds and have 300 watts internal loss. Therefore a study is under way to reduce the weight. A small percentage gain will save many pounds. One direction of study is explained briefly.

The three phase primary power would be rectified directly using SCR's (silicon controlled rectifiers) which would be operated in a phase controlled configuration. This would produce a highly efficient supply as there is no loss-producing series or shunt d.c. regulator. The 220 volt output would be filtered with passive devices and then "chopped" at the Radar Pulse Repitition Frequency. By chopping at the P.R.F. the power supply ripple would coincide with the P.R.F. spectral lines thus reducing the requirements on the filtering at the chopped frequency.

The P.R.F. is relatively high $\approx$ 7.0 K.C and a corresponding voltage step up transformer will weigh much less than its 400 cycle counterpart. This configuration shows promise of reducing the weight from 35 pounds to 15 pounds. The difficult problem lies in maintaining efficiency as the chopper transistors do add considerable loss.

Westinghouse has considerable experience in the field of high power, solid state, low frequency, a.c. power generation. This aspect will be studied and a decision made as to the power supply configuration within the next month.

2.3 RECEIVER

2.3.1 Preselector (Figure 2-14)

2.3.1.1 Cross Modulation

The proposed receiver was mechanized on the basis that interfering signals would be smaller than the clutter return. Conventional transistorized front-end techniques could have been employed to minimize the cross modulation by interfering signals without sacrificing Noise Figure. With interference greater than clutter it is necessary to employ extraordinary techniques to meet the requirements.

A mathematical theory is being developed to predict the amplitude of cross-modulation products resulting from off-band signals mixing with clutter components and/or with a local oscillator. So far this theory reveals that the most damaging set of cross products results from even order cross modulation. This clearly indicates the use of push-pull amplifiers and balanced mixers and gateswhere interference signal levels would be highest (e.g. First Mixer, Post-Amplifier, Snuffer, and First IF Amplifier). Hot carrier diodes were selected for the mixer because they have inherently good balance. It is then necessary to have a filter ahead of the high level stages to reduce the level of the interference which would produce odd order cross modulation. This filter must also provide some attenuation to the interference which would produce even-order cross modulation since the push-pull amplifiers and balanced mixers can be only counted on for a limited amount of common mode distortion suppression.

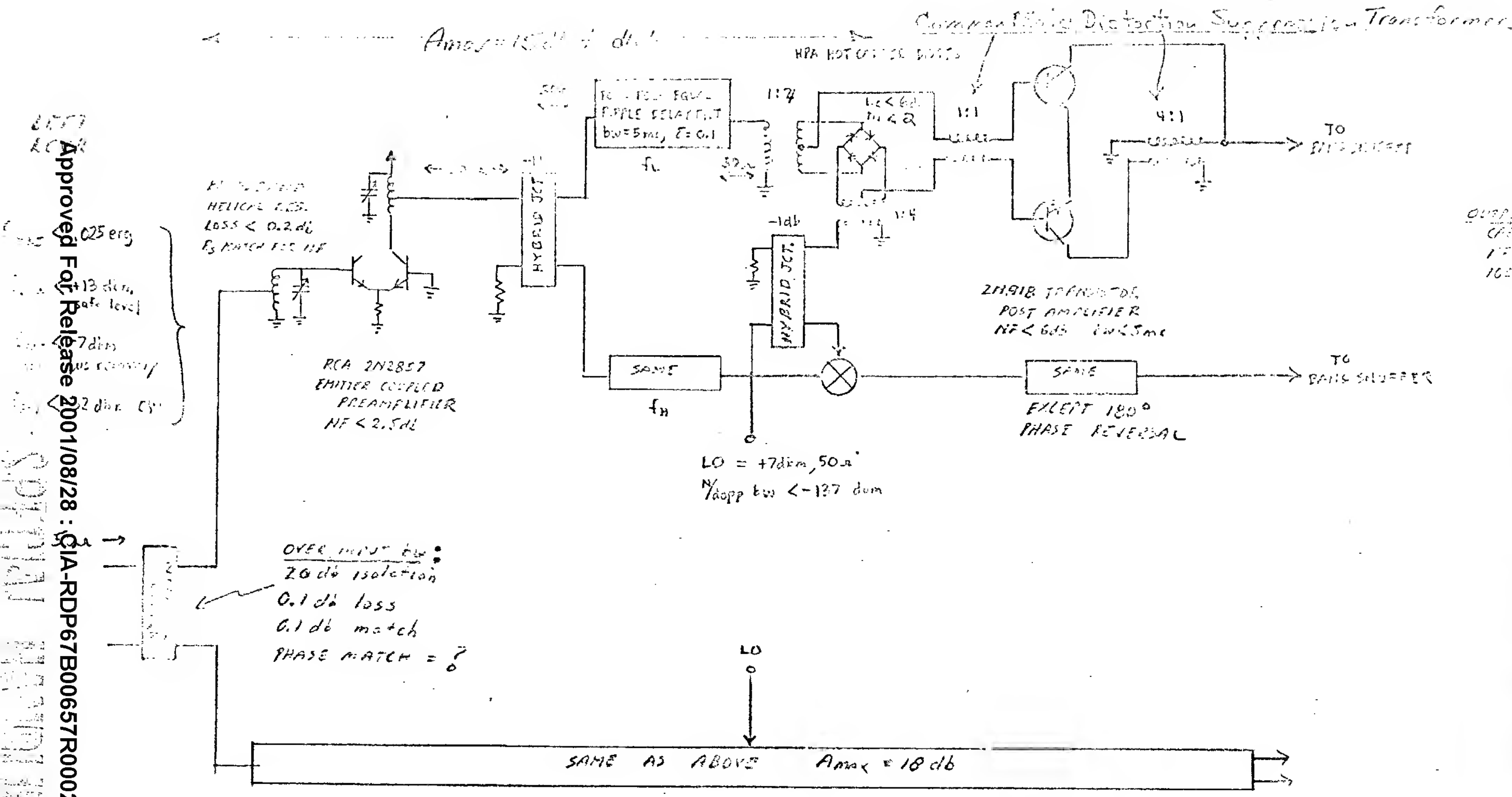

POWER GAINS GUSTED

Σ NOISE FIGURE < 3db

$\frac{\text{CROSS MODULATION}}{\text{NOISE IN DOPP. BW}} < \frac{1}{1}$

$\frac{\text{INTERMODULATION}}{\text{NOISE IN DOPP. BW}} < \frac{1}{1}$

REF 5/13/64 SPEC FOR TRANSMITTER LEAKAGES

Figure 2-14 Preselector

With the transmit frequency at one end of the band, significant cross products can be produced by interference at the other end of the band. Therefore, it is necessary to tune the filter. When the interfering CW signal is less than -32 dbm cross modulation product should not exceed the noise in a doppler bandwidth. Preliminary studies indicate that this requirement can be met with a two position tuned filter, or with two separate filters as illustrated in figure 2-14. The feasibility of making this filter tunable is under study, and the mechanization will be changed if at all possible. This would save the hardware which presently must be duplicated for the high and low channels. The filters should provide reasonably constant time delay over their passband to guarantee fast recovery from the various frequency transmitter pulses, (see figure 2-15).

Further advantage is taken of the reasonably constant time delay by putting 180° phase reversal in one of the port amplifiers so that the transmitter leakthru pulses will tend to cancel out.

It should be noted that the preamplifier is not as sensitive as the above to cross modulation since a large L.O. signal is not present, and since the interference and clutter are at lower levels. Some filtering is required, but this is provided by the antenna bandwidth.

2.3.1.2 Intermodulation

The intermodulation problem is most severe at the mixers, since here the signal levels are the highest. Any attempt to

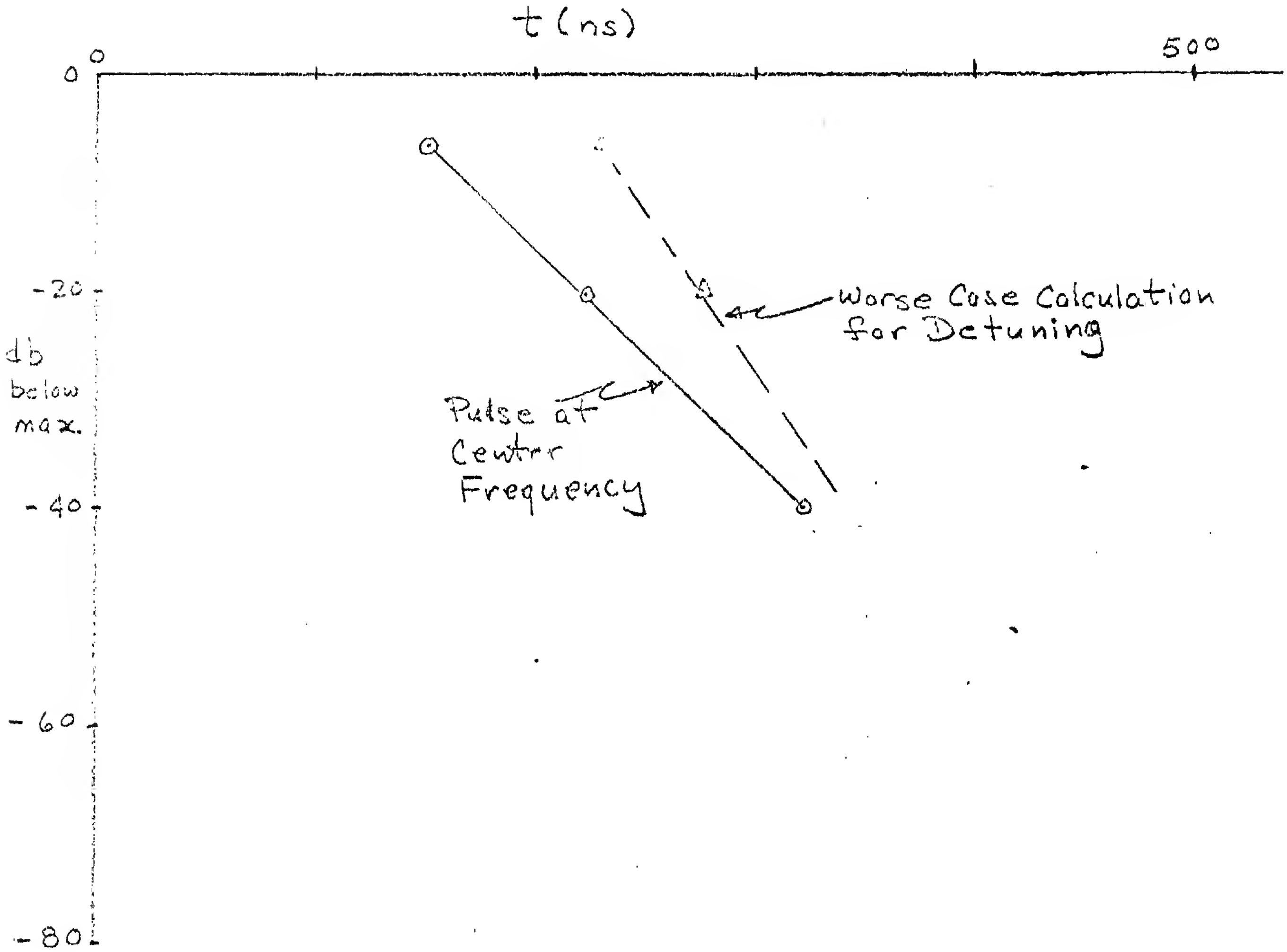

Figure 2-15 Pulse Decay In Preselector Filter

linearize the mixers by using feedback results in greater conversion loss, which degrades noise figure. This problem is made even more severe due to the anticipated broad bandwidth over which the clutter amplitude is maximum. Preliminary calculations indicate that maximum peak clutter levels in one doppler bandwidth result in intermodulation comparable to noise.

If increased clutter levels have to be handled or if final calculations reveal problems, then phase cancellation mixers would have to be used. (i.e three double balanced mixers spaced at 120°).

Test methods have been devised to measure the small intermodulation product amplitudes. The measurements require 20 db more dynamic range than those performed in the past. A special low noise measurement receiver has been procured for these measurements.

2.3.1.3 Noise Figure

The overall noise figure is to be 3 db and the noise figure of the first amplifier stage should be in the area of 2.5 db. The transistor selected for the first stage is the 2N2857. Available information indicates that with optimum source impedance and collector current this transistor may be suitable. An emitter coupled amplifier has been chosen because it will have a larger linear dynamic range and thus produce smaller intermodulation products. A measurement set up is being prepared for the purpose of determining the noise figure and the optimum source impedance and collector current.

If measurements indicate that the 2N2857 will not meet the noise figure requirement then the more expensive TIX3016 can be used. The information on this transistor indicates that the 2.5 db noise figure definitely can be obtained.

It is anticipated that the hot carrier diode balanced mixers will have low conversion loss and excess noise ratio due to the low knee of the diodes and the elimination of charge storage. Tests are in process to determine the mixer performance. L.O. Noise is controlled to keep the degradation of noise figure to a minimum.

After the post-amplifier the noise contributions become less significant to the over-all noise figure, and so no particular problems are anticipated.

2.3.2 Second IF Converter (Figure 2-16)

The effect of interfering signals lying very close to our passband would ordinarily be very slight. However, if a conventional square Bang-Snuffer is used, the interfering signal spectrum would be spread so that energy is at frequencies spaced at multiples of the prf. With large interfering signal levels these sidebands would excessively degrade system performance. Therefore the Bang-Snuffer is designed to have smoothly changing on and off characteristics. The "Sloughing Snuffers" keep the sidebands of interfering signals below noise if their edges have a transition shaped as a $\sin^2$ function, changing from on to off in more than 4.2μs. It is necessary to clamp the control voltage to a fixed value in the ON or OFF positions so that power supply ripple will not modulate signal or leakthru.

SPECIAL HANDLING

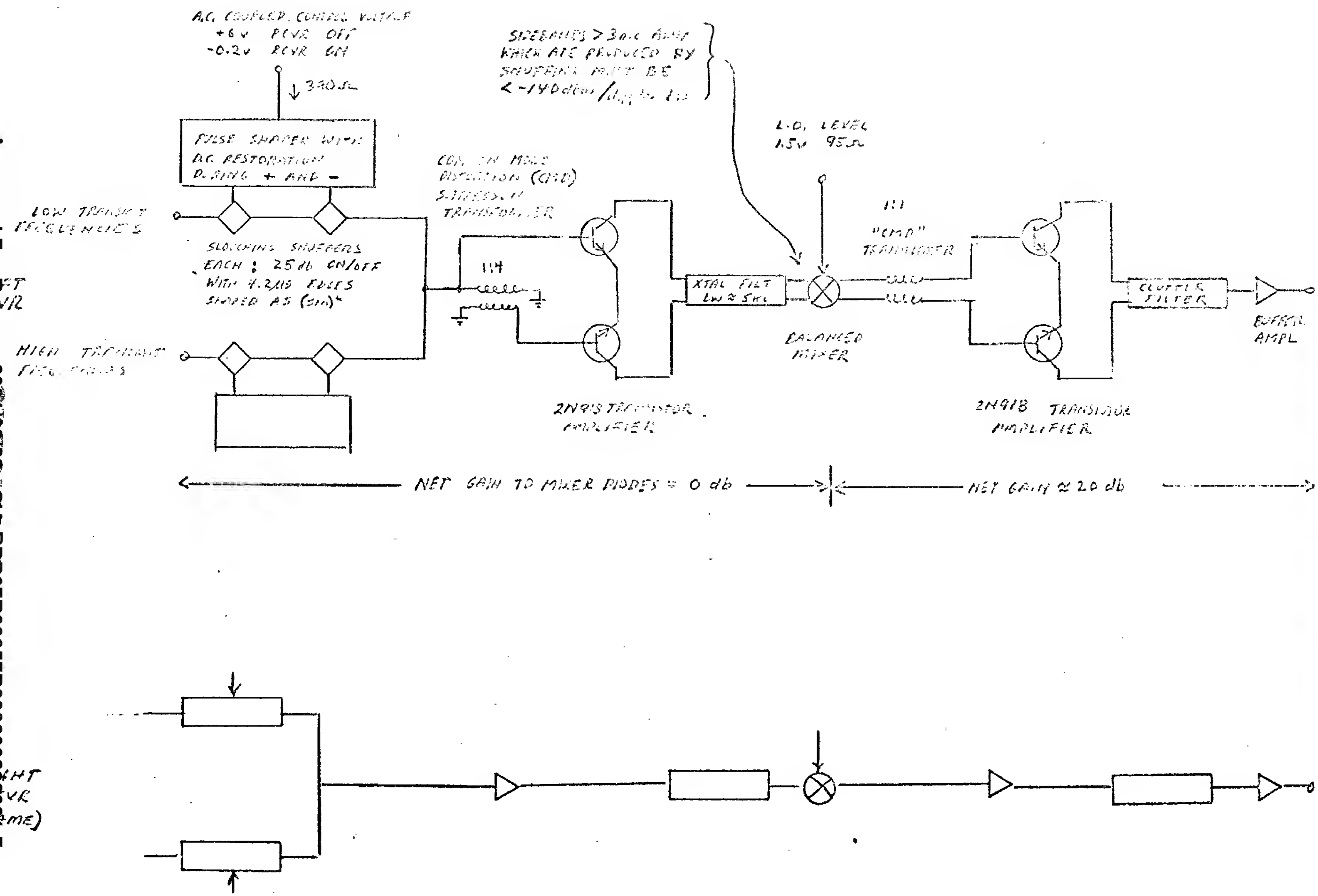

ΣNoise Figure <6 db

CROSS MODULATION AND INTERMODULATION < NOISE IN DOPPLER bw.

Figure 2-16 Second I.F. Converter

2.3.3 Main IF Amplifier and Converter (Figure 2-17)

The second and third IF now contain an AGC loop. It is anticipated that the signal and the clutter dynamic ranges would be greater than those anticipated in the proposal, and the AGC will enable the receiver to function satisfactorily over these ranges.

The block diagram of figure 2-16 shows that each receiver (left and right) has two IF amplifiers, one to drive the clutter tracker and one to drive the doppler filter bank. Although the amplifiers are identical, they are separate because it is anticipated that the AGC requirements for the two functions will be different.

Preliminary studies of this section of the receiver showed that 110 db of gain with 20 db of AGC range would be required. Because of the difficulty of controlling the gain of higher power amplifiers, it was chosen to control only the first stages, leaving the last higher level stages uncontrolled. Methods of varying the gain of the low level stages without exceeding the intermodulation requirements are under investigation. Intermodulation requirements are not as severe in this part of the receiver because the large clutter signals are not present. With maximum output the third order intermodulation products should be at least 50 db below the desired output signal with the amplifier at full gain, but these products may increase slowly as gain control is applied.

In mechanization of a 70 db "jump snuffer" (transient gate), a balanced configuration is used to assure that the

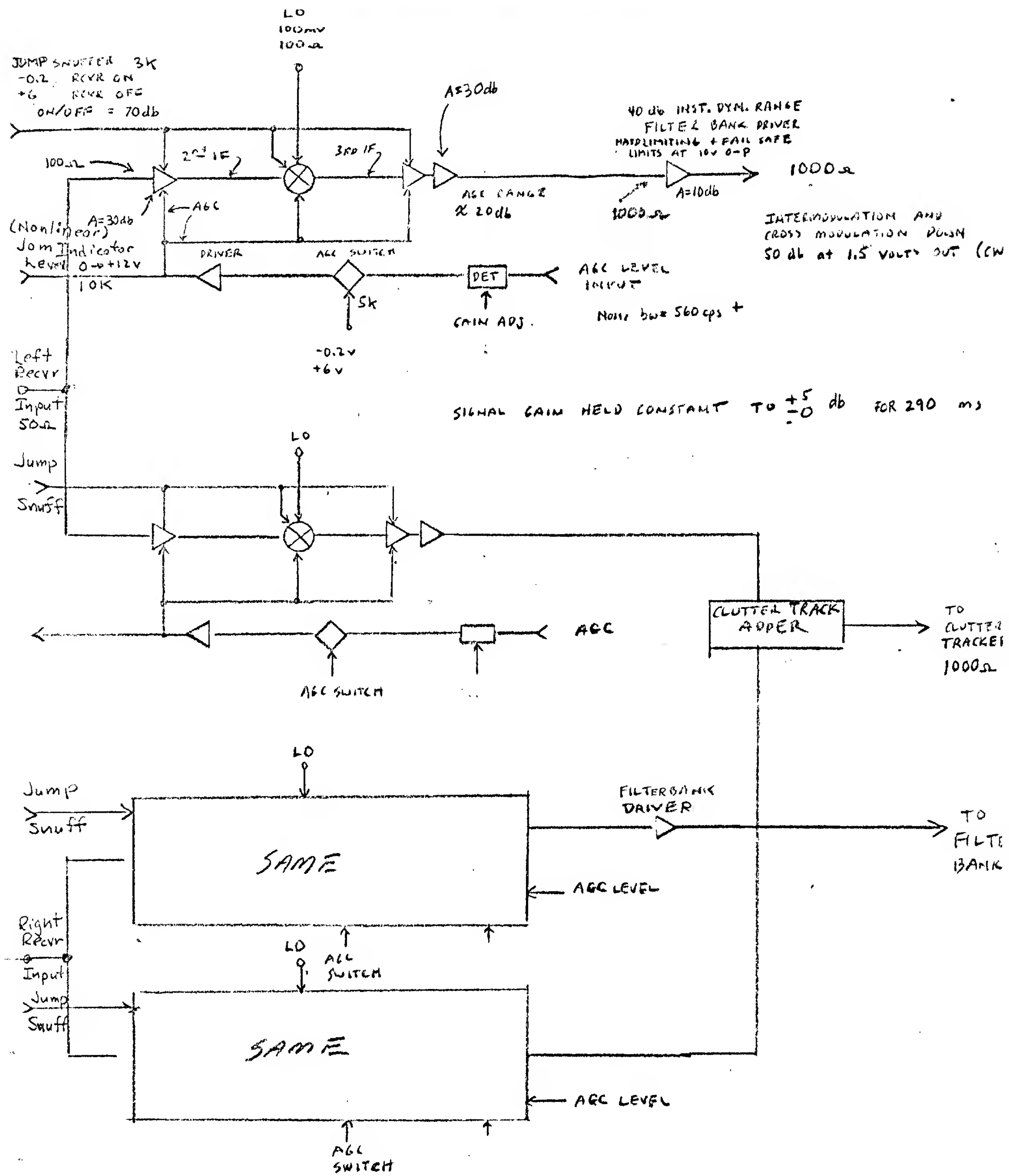

Figure 2-17 Main IF Amplifier and Converter

transient produced by the gate itself will not seriously affect the system.

The AGC loop uses a delay (level threshold) and a time sample-memory feature. The "sample-store" function is implemented by an AGC detector having two different time constants which are switched by a "sample-store" gate pulse which is originated in another part of the system.

Because of the potential size and reliability advantage of integrated circuitry, use of Westinghouse functional blocks is being considered for most of the functions in this section of the receiver. Preliminary circuits have been designed and constructed for many of the stages and experiments have demonstrated the feasibility of this approach. Detailed design is proceeding and a preliminary concept has been reached.

2.4 DATA PROCESSOR

The Data Processor serves as system operation sequencer as well as performing specific functional operations.

2.4.1 System Operation Sequencing

System operation sequencing is shown in flow chart form in Figure 2-18. All decisions, indicated by rounded blocks, are executed in the data processor. Elapsed time of operational cycles is determined by blocks indicated with an asterisk. Note that processing of threshold detections for target recognition proceeds simultaneously with scanning of the filter bank and does not impose a requirement on cycle time. The symbols n and x represent flip flops.

2.4.1.1 Data Processor Functional Operations

Functional operations performed by the Data Processor are described with reference to the functional block diagram shown in Figure 2-19.

2.4.1.1.1 Timing Signals

The Central Clock Generator accepts the output of a stable crystal controlled oscillator and generates various subharmonics of the crystal frequency through a binary counting process. Various states of the counters are decoded for use as timing signals.

A set of four pulses is sent to the RF subsystem for each RF pulse transmitted. Either of two repetition rates are selected for this set of pulses. One of the four pulses at the lower repetition rate is also sent to the filter bank to control events during the integration period.

Another set of pulses synchronize the filter bank interrogator with the centroiding register, the data register, and the data comparators. Other clock pulses are provided in too great profusion to be shown in Figure 2-19.

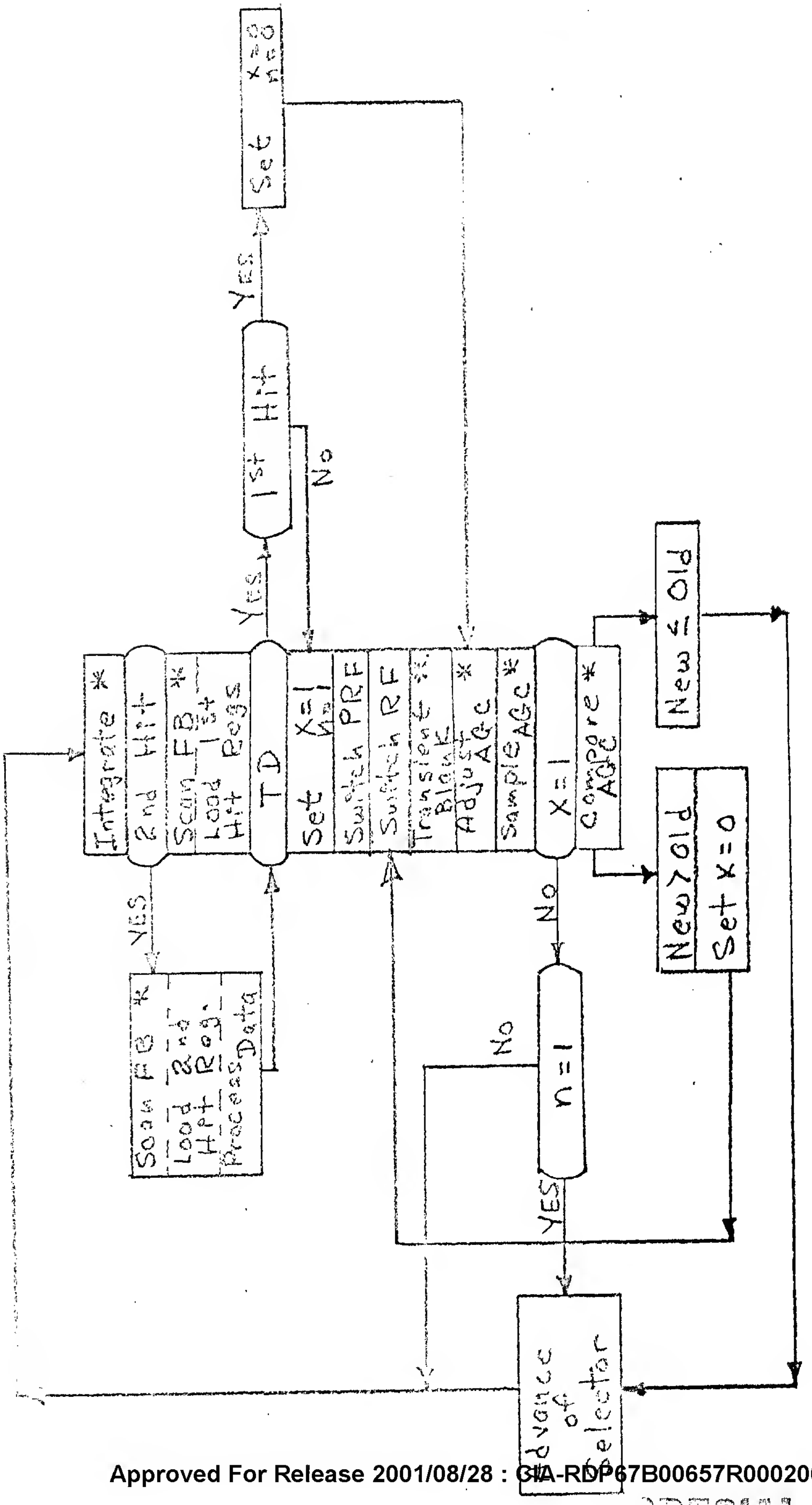

Figure 2-18 System Operation Sequencing

2.4.1.1.2 Selection of Transmitter Frequency

As indicated in Figure 2-18, the RF is periodically switched and the resulting AGC voltage is compared with that obtained by use of the previously selected RF. The AGC processor converts the analog AGC voltage to digital form and compares it with the stored value from the previous sample. The RF selector contains two registers which retain identities of the currently selected RF and the next to be selected RF. The identity of the currently selected RF is transmitted to the RF subsystem on a "one-hot" line basis. The same information is transmitted to the Velocity Multiplier Amplifier gain switches on a "one-hot" line basis.

2.4.1.1.3 Processing of Threshold Detections

During filter bank interrogation periods the centroiding register receives threshold detections and counts the number of such detections which are derived from successive filter positions in the filter bank. When a miss occurs after a string of threshold detections, a "1" is set into a bit position in one of the data registers which corresponds to the value of the count in the centroiding register. The centroiding register is reset to zero and counting will resume with the next threshold detection. The bits in the data register are shifted in synchronization with the filter bank scan. Hence, at the end of filter bank interrogation, the pattern of "1's" in the data register represents the centroided values of the strings of threshold detections from the filter bank.

The centroiding register will recycle and set data at a prescribed maximum count if the number of threshold detections in a string exceeds the prescribed maximum number.

Operation of the Data Register Selector (DRS) and Hit Detector (HD) can be readily understood by assuming that the first threshold detection from the filter bank was obtained on the Nth interrogation. On all previous cycles, both PRF and RF were switched each cycle as indicated in Figure 2-18. Also, the DRS had selected data registers L (N) and R (N) to receive centroided values each cycle.

On the Nth cycle, at least one threshold detection was received and the centroided values(s) stored in L (N) or R(N). The Hit Detector then causes the DRS to select L (N + 1) and R (N + 1) to receive data during the next filter bank interrogation. Simultaneously, switching of RF and PRF is inhibited. At the end of the (N + 1)st cycle, the DRS reverts to selection of L (N) and R (N) for the (N + 2)nd cycle and both PRF and RF are switched.

Centroiding results in quantization units half as large as those of the noncentroided data, hence the registers L (N) and R (N), which store data for one system cycle, consists of approximately twice as many flip flops as there are filter positions in the filter bank. The lengths of L (N + 1) and R (N + 1) are determined by data processing criteria rather than storage requirements since data processing proceeds simultaneously with the (N + 1)st scan of the filter bank. L (N + 1) and R (N + 1) consist of approximately one third as many flip flops as L (N) and R (N).

Each comparator circuit (left and right) consists of a number of logic gates interconnected in such a way as to detect certain prescribed bit patterns as the contents of the register L (N) and L (N + 1) [or R (N) and R (N + 1)] are shifted past. Target detection criteria are shown in Figure 2-20.

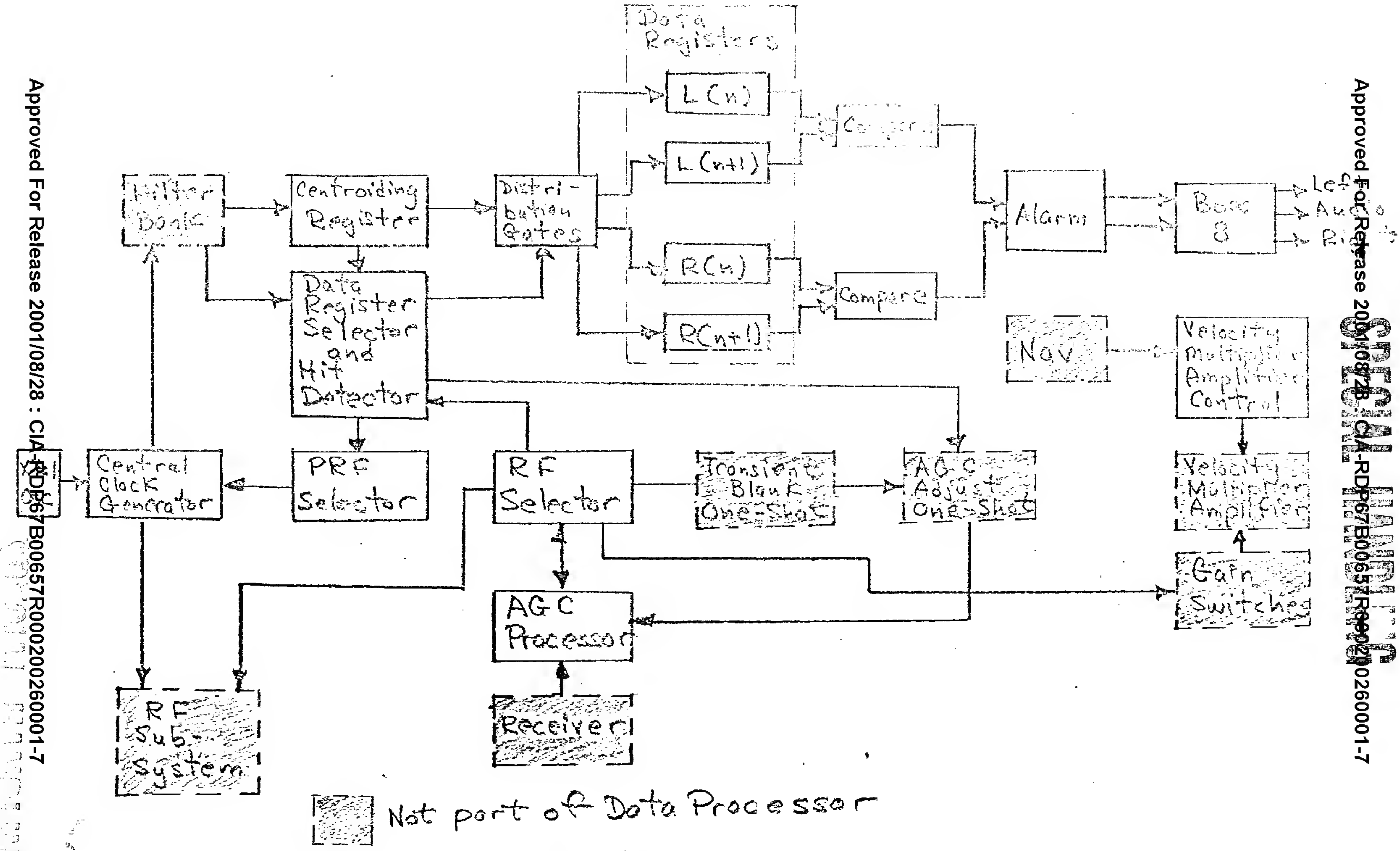

Figure 2-19 Data Processor Functional Block Diagram

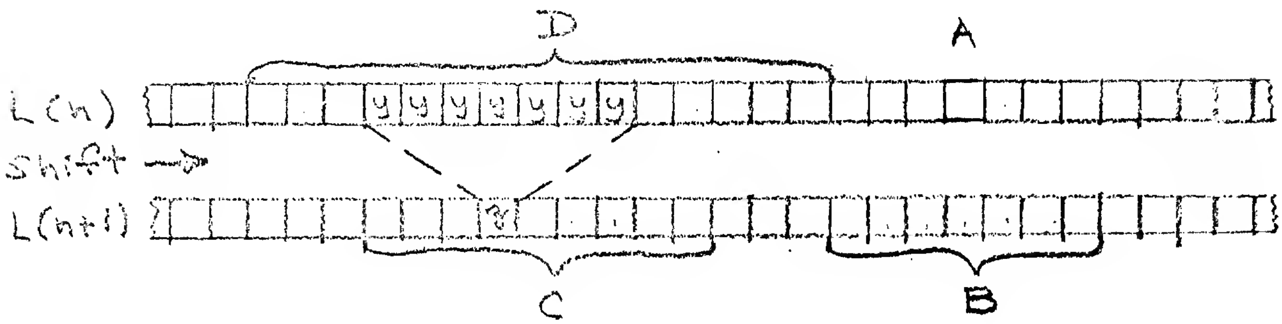

Target Criteria

A	B	C	D	Target
0	X	X	X	No
1	X	0	X	No
1	0	1	0	Yes
1	0	1	1	Yes
1	1	1	0	Yes
1	1	1	1	No*

* No only if the "1" in D bears a specific relationship to the "1" in C. Thus, for a "1" in position z in C the specific relationship would be satisfied by a "1" in D only if it were in one of the positions indicated by the symbol y.

Figure 2-20 Target Criteria

2.4.1.1.4 Alarm

In the event that either comparator or both detects a prescribed bit pattern, the alarm circuitry will be activated. If both left and right alarms are activated as the result of the same filter bank interrogation both alarm lights will be turned on and an audio tone will be generated in the earphones of the crew for a period of 30 seconds. If only one alarm is activated the corresponding light and the audio tone will be turned on but the other alarm will be inhibited for the 30 seconds duration of the first alarm.

The block of Figure 2-19 labeled Alarm contains the 30 second timer and the inhibit circuitry. Box 8 contains the audio signal generator and circuitry for conversion of signal level from that of the system to that of the vehicle.

2.4.1.1.5 Velocity Multiplier Amplifier Control (VMAC)

The VMAC accepts velocity from a doppler navigation equipment in the form of a 12 bit binary word transmitted in serial with the most significant bit first. Ones and zeroes are represented by positive pulses on separate lines. Positive pulses simultaneously on both lines in the 13th bit position indicate end of transmission. Both pulse amplitude and pulse width are converted to values compatible with system mechanization.

In addition to the signal conversion circuitry, the VMAC contains three 12 bit registers, a 12 bit D/A converter, and some miscellaneous logic. One 12 bit register receives the converted data from the navigation equipment. A second 12 bit register holds the digital value for conversion. The third 12 bit register serves as an exchange medium between the first two. Navigation data is transferred to the exchange

register by the end of transmission signal. New data is entered into the holding register only at time of RF switching in order to not put transients into the system. The miscellaneous logic assures that both transfers do not occur simultaneously.

2.4.2 Mechanization

The Data Processor will be mechanized utilizing Integrated Circuits packaged in TO-5 12 pin cans mounted on double sided printed circuit boards. The boards will be special purpose in order to increase the packaging density.

2.4.2.1 Circuits

Microelectronic Integrated Circuits (MIC) are utilized wherever possible. DTL type MIC blocks were selected and are furnished by Westinghouse Molecular Electronics Division. The MIC blocks used are WM213T, WM201T, WM211T, WM210T, WM224T. The Data Processor uses approximately 500 12-pin cans of MIC circuits in addition to the conventional components used in the 12-bit D/A converter and the 4-bit A/D converter.

2.4.2.2 Packaging

The Data Processor will be packaged by utilizing ten different types of printed circuit boards containing an average of 45 cans per board. The block diagram, Figure 2-19, is divided into boards as shown in Table 2-2.

2.4.3 Progress to Date

A. Sybsystem Design 90% complete

B. Logic Design 90% complete

C. Layout completed for five of the ten types of boards

D. Taping of one board complete

E. Subsystem test tool designed and being fabricated.

F. All parts ordered for breadboard

G. 50% of integrated circuits for breadboard received and tested.

Table 2-2

Data Processor Board Divisions

Board Type	Function
1	RF Selector, Alarm Circuitry
2	Data Registers
3	Data Registers
4	Data Processor
5	AGC Processor, RF Advance, RF Select, PRF Select
6	Central Clock Generator
7	Data Register Selector, Hit Detector, AGC Process Control
8	Centroiding Register
9	Velocity Multiplier Amplifier (VMA)
10	VMA D/A Converter

2.5 CLUTTER TRACKER AND VIDEO CIRCUITS

2.5.1 Clutter Tracker Mechanization

The clutter tracker mechanization is proceeding substantially as planned in the proposal. The only changes of significance are 1) the digital velocity information-to-analog voltage for the clutter track oscillator, 2) the clutter track oscillator, 3) all frequencies and 4) various gating circuits. In addition, the exact specification of the clutter track audio amplifier will not be known until a better model of the clutter is available as an outgrowth of the flight tests in progress.

2.5.2 Clutter Tracker-Navigator Interface

In the proposal, the interface between the external doppler navigator and the clutter track VCXO was a stepping motor controlled by four wires from the doppler navigator. The stepping motor was mechanically connected to a potentiometer which was supplied with a D.C. voltage proportional to the transmitter frequency. Such a mechanization produces a D.C. voltage on the potentiometer arm proportional to true doppler to control the clutter track VCXO.

Subsequently, it has been determined that changes in the velocity information from the doppler navigator occur in real time; this conflicts with the system requirement that oscillator frequencies change only in a particular time slot set aside for PRF and frequency changes. It is also desirable from a reliability standpoint to have an all electronic interface.

The interface has therefore been changed to a gated digital-analog converter supplied by a 12 bit serial velocity word as described

in the data processor section of this report. The analog voltage is fed to an operational amplifier, the velocity multiplier, with feedback controlled by the same lines which select the transmitter oscillator frequencies. Thus, the output of the velocity multiplier is equivalent to the voltage at the arm of the potentiometer in the original mechanization with the important exception that it is now buffered from unsynchronized changes in velocity data.

2.5.3 Velocity Track VCXO

The mechanization of the velocity track VCXO is the most difficult part of the clutter track circuits because of simultaneous requirements of linearity over a wide range, stability, spectral purity, and vibration input. The mechanization in the proposal obtained an output around 187 KC by beating a VCXO and a fixed oscillator in the 1 mc range. Revised system requirements have changed the clutter track VCXO output to around 975 KC, with the deviation remaining 1.6 KC. A number of mechanizations are possible:

1. Direct generation
    a. Open loop VCXO at 975 KC
    b. Frequency track loop
    c. Digital control by selection of capacitors, etc.
    d. Several open loop VCXO's in 975 KC range
2. Heterodyne generation
    a. VCXO and fixed oscillator in 15-20 mc range.
    b. Audio VCO and fixed oscillator in 975 KC range.

Detailed specifications for this VCXO have been submitted to several

suppliers. It is intended to select one external supplier and carry a back-up program at Westinghouse using a different approach.

Method 2a appeared to be the best choice and a 20 mc VCXO was built having the required linearity; however, with the VCXO in a Statham Chamber for temperature control, the long term stability was inadequate. Tests have been discontinued on this oscillator until a choice of external supplier has been made, and the present effort is toward perfecting a noise measurement technique so that data can be obtained on spectral purity (particularly) in the vibration environment.

2.5.4 Velocity Multiplier

The velocity multiplier and summation amplifiers have been designed and preliminary tests made. The precision resistors have been ordered and final tests will be made when the resistors are received.

2.5.5 Scan VCXO

The scan VCXO specification has been submitted to several suppliers. This unit is within the state-of-art and no problem is anticipated in obtaining it as a purchased part.

2.5.6 Fixed Oscillator

The 975.4 KC fixed oscillator specification has been submitted to several suppliers, and a design has been tested at Westinghouse. No problem is anticipated; the oscillator will be purchased externally if the cost is attractive.

2.5.7 Mixers

Preliminary designs exist on the mixers. A balanced transformer is to be selected before breadboards are built. Work on the various filters has been deferred.

2.5.8 Clutter Spectrum

Some calculations have been made to establish the audio amplifier, track detector and integrator requirements. These calculations, based on idealized clutter spectrum and the proposed clutter filter response shapes did not yield adequate information to complete the design. Therefore, when current studies, including flight tests, yield a more accurate model of clutter, the design will be resumed.

2.5.9 Gating Circuits

The gating circuits for the third IF section of the receiver have been designed and tested. The board containing these circuits is in drafting. Gating circuit designs for the front end of the receiver and for the transmitter exist but are expected to change from time to time as the final form of the receiver and transmitter design evolves.

2.6 LOW VOLTAGE POWER SUPPLIES AND SPECIAL TEST EQUIPMENT

2.6.1 Low Voltage Power Supplies

2.6.1.1 Design Changes Since Proposal

The basic scheme of low-voltage d-c power distribution has been revised. Instead of having the unregulated power supplies in one location with individual voltage regulators located in each unit, all of the voltage regulators (with one exception) will be located on the same pallet as the unregulated sources. This revision was made because a total of 8 different voltages will be distributed to the various units over 21 different lines, there being multiple users of most of the voltages. Thus, with the present arrangement, only 8 separate regulators are required whereas 21 separate regulators would have been required for the original scheme.

The basic principle that is being followed in the d-c power distribution system is that each voltage source will be connected to each unit by a separate pair of lines, one of which will be the ground return. These lines will be shielded, twisted pairs with the shield connected to the unit chassis ground at one end and to the power supply chassis ground at the other end. Both power supply terminals will be isolated from the power supply chassis. The common, or ground return, line will be firmly grounded at the unit by connection to the chassis ground of that unit. This principle is illustrated by the block diagrams, figures 2-21 and 2-22. It is believed that this method will reduce crosstalk and stray pickup on power lines to a negligible level.

The one exception to the regulator location arrangement is the data processing unit. The regulator for this unit will be located

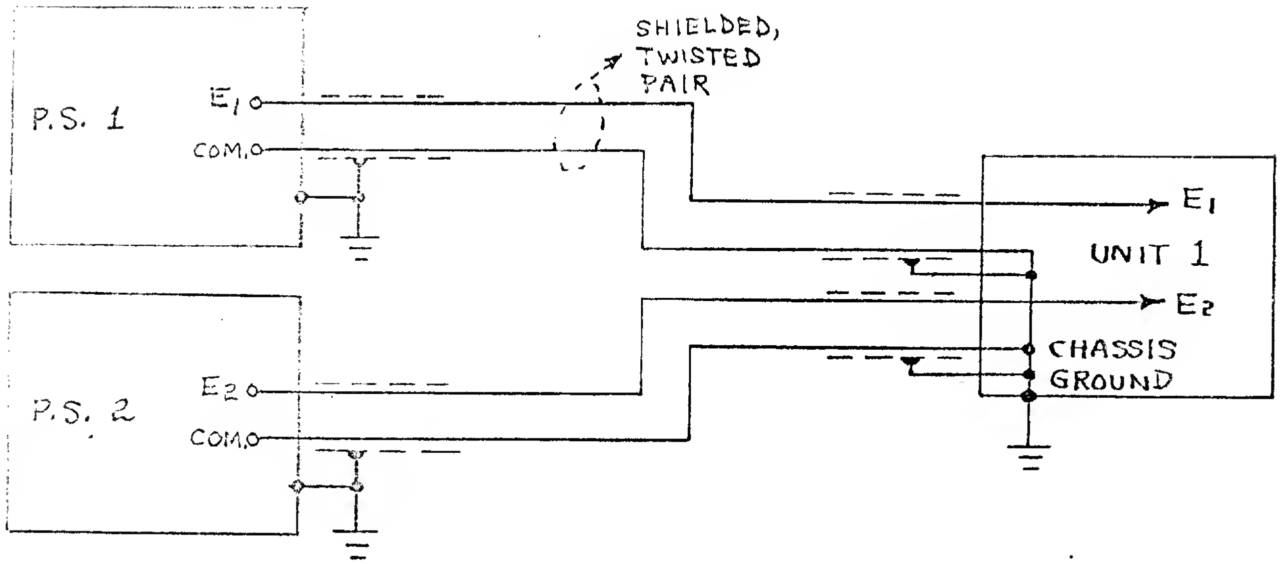

FIGURE 2-21 POWER DISTRIBUTION WIRING WITH MULTIPLE POWER SUPPLIES FEEDING INTO THE SAME UNIT.

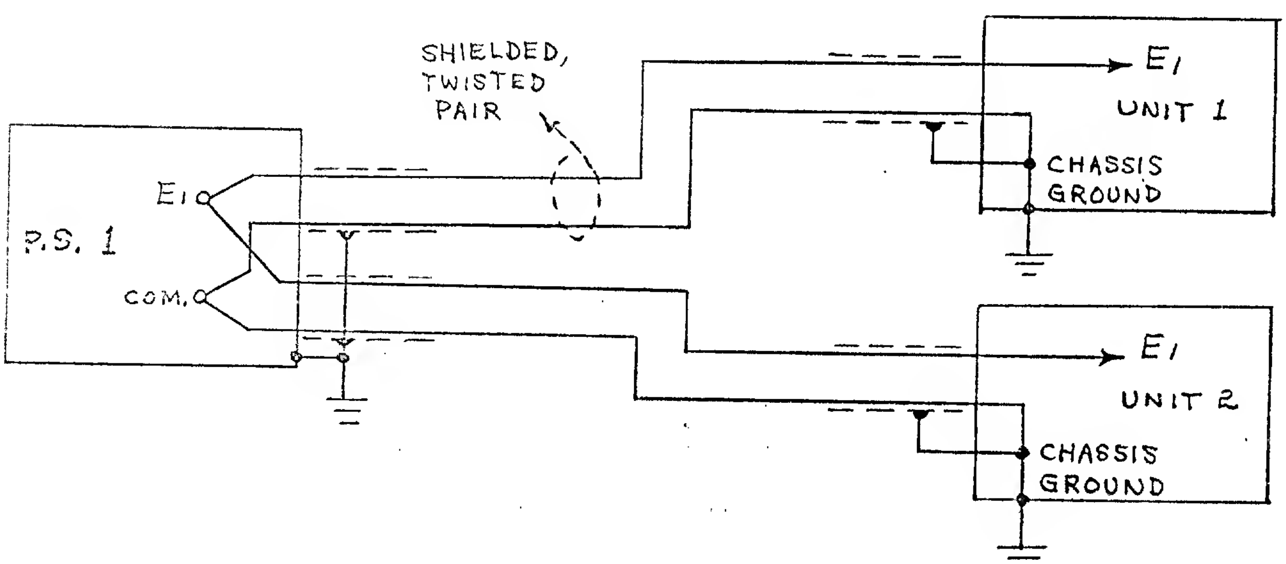

FIGURE 2-22 POWER DISTRIBUTION WIRING WITH ONE POWER SUPPLY FEEDING INTO MULTIPLE UNITS.

within the unit itself, thereby eliminating radiation from power lines carrying pulse currents that are typically found in digital equipment.

2.6.1.2 <u>Description and Characteristics</u>

A completely separate power supply, consisting of a transformer, rectifiers, and a regulator has been designed for the sole purpose of providing d-c power for the crystal ovens. The primary a-c input to this supply is the 3-phase a-c line, so that this supply will be energized whenever the a-c power is present. This will permit oven warm-up sufficiently in advance of actual system operation.

At the present time, the intention is to use no passive filtering between the rectifiers and the regulator inputs (other than transient voltage spike suppressors). The voltage regulators designed for this system have greater than 80 db of ripple suppression over the frequency range of interest. The regulators themselves will therefore be used to provide active ripple filtering. In this manner, 8 filter choke coils will be eliminated, resulting in a very considerable reduction of power supply size and weight.

The regulators will provide better than ±0.2% voltage regulation over the full range of load currents, temperature, and normal input voltage specified. They will be completely overload and short-circuit proof, with operation in the overload region between full-load current and short-circuit clearly defined as to output current, voltage, and element dissipation for all values of load resistance down to zero ohms. All overloads can be sustained indefinitely with no damage to the regulators. Output voltage recovery after an overload is completely automatic,

and requires approximately 20 milliseconds. Each regulator will be designed for a specific value of full load current; any reduction in load resistance beyond this point will result in a reduction of both load voltage and load current. Consideration has also been given to the possible large input overvoltage transients that could occur. If such a transient occurs, a circuit will reduce the regulator output current to zero for the duration of the time that the input voltage is above a given level. This level will of course be appreciably above the normal operating range of input voltages.

2.6.1.3 Present Status of Low Voltage Power Supplies

The basic circuitry to be used in all of the voltage regulators has been developed, and preliminary tests have been made. The component layout for the prototype regulator boards is nearly complete. One of these prototype boards will be constructed within a week, and more detailed tests of the circuit will be started at that time. Information on the low-voltage power supply transformer requirements is expected to be complete within one week, at which time the transformer designs can be started.

2.6.2 Special Test Equipment

A study has begun to determine the detailed system requirements of the special test equipment. No detailed design work on this equipment has been made to date.

2.7 FILTER BANK AND INTERROGATOR

The present concept of the filter bank reflects some changes from the originally proposed system. These changes have resulted after further studies of system requirements. Work is currently progressing in the design phase as well as laboratory investigation of special techniques in the planned mechanization. Different packaging philosophies are being evaluated to arrive at the best mechanical configuration. Approximately 80% of the signals at the filter bank interfaces are completely defined.

The deviations from the proposed system are categorized below according to functional requirements of the signal processing equipment.

2.7.1 Channelization of the Doppler Spectrum

The number of discrete frequency detectinn channels for each of the two filter banks (left and right banks) is now established at 40 instead of the originally proposed 25. Quartz crystal resonators will be used in a 3-pole filter having Butterworth characteristics. The 3-pole "shared" technique involves the sharing of two of the three crystals per channel with the two adjacent channels. The bandwidth at crossover of adjacent filters is now 14 cps, and the 3 db bandwidth is 16.2 cps. The filter was initially proposed as a 2-pole filter having a 3 db bandwidth of 20 cps. The change to 3-pole filters provides greater resolution of targets due to steeper skirts of the attenuation-frequency response.

A specifications has been written for the crystals and a purchase order has been placed for crystals to be used in the breadboard system.

2.7.2 Envelope Detection and Integration

The standard approach in the mechanization of a filter bank frequency detection channel includes amplification of the filter output to obtain a signal commensurate with detection requirements and the subsequent envelope detection performed by an amplifier and detector in each channel. A different philosopy has been adapted in this system wherein the filter outputs and post-detection integrator inputs of each channel are multiplexed to a single amplifier and detector per bank. The advantages of a multiplexed system are primarily improved tracking stability from channel to channel and fewer adjustments necessary. A trade-off of linear network elements is a standard approach for switching elements in the multiplexing scheme and may be considered as an advantage because of reduced power consumption and lower component count. The bandwidth of the filter and number of channels involved make the multiplexing technique feasible. According to sampling theory, the minimum rate of sampling a signal to insure recovery of the unsampled information without distortion is twice the highest signal frqeuency in the sampled information. For a 3 db bandwidth of 16.2 cps the sampling frequency should be at least (2) (16.2) = 32.4 cps. A sampling rate of 75.7 cps will be employed for the multiplexed filter bank.

The post-detection integration function is being mechanized with a capacitor which will act as an ideal integrator except for negligible effects of capacitor leadkage. The effectively ideal integrator is based on use of a detector output stage which functions as a current source. This technique is feasible since the integrator will be "dumped" or discharged and clamped after interrogation of the integrator following each integration period. The integration time is 290 milliseconds,

as compared with the initially proposed 1/3 second.

The amplifier of the multiplexed frequency detection channels will have an AGC loop to provide +10 db, -30 db, of gain control. This range of gain control is required to maintain a constant average noise level at the amplifier output. The average noise input to the filter bank from the third IF will not be constant bec use of the "memory" AGC techniques employed in the third IF. The control of the AGC amplifier is achieved by use of a reference channel which consists of a wide band-pass filter multiplexed to the amplifier and detector utilized by the 40 normal channels. The detected output of this channel, after filtering with a low-pass filter which has a response commensurate with that of a 3-pole band-pass filter, is used as the AGC signal for the amplifier. The AGC amplifier will have an instantaneous dynamic range of 20 db to handle signals and noise impulses.

2.7.3 Commutation or Interrogation

The sequential readout of the post-detection integrators will be accomplished with an electronic scanning device. Present plans are to use a magnetic core-transistor scanner since this type of mechanization is most compatible with the multiplexed filter bank system. The magnetic core scanner particularly satisfies the requirement of isolated control signals for bilateral switches employedin the multiplexing scheme. The news of a recent release of specifications on a field effect transistor that has a significantly improved saturated voltage drop characteristic will be investigated within the next reporting period. Ultimately this type of device is highly desirable as a replacement of the chopper transistors used as switching elements, since

an isolated control signal is not required and a microelectronic scanner then becomes more advantageous.

The interrogation process will be carried out by the scanner at a 44.52 kc rate (22.5 usec/step). Both left and right banks will be scanned twice, position for position, so that a relative comparison may be made of the outputs of corresponding channels. In the first interrogating scan of the post-detection integrators decisions are made regarding the presence or absence of a target in the left bank. The second interrogating scan provides the same information for the right bank. The decisions about targets are presented to the Data Processor unit for further processing.

The sampling of signal information will be mechanized using the same scanner as used for interrogation, except that the scanning rate will be 6.36 kc. This time-sharing feature reduces overall system hardware. The logic and control circuits of the filter bank will be mechanized to a large extent with microelectronic circuits.

2.8 ACTIVE SUBSYSTEM PLANS FOR NEXT REPORTING PERIOD

During the next month great stress will be placed on completing all long lead item specifications and placing firm orders for all components for the first engineering model. Plans for system testing and any special test equipment required will be given the full attention of our system analysis and integration group this month.

Some of the hardware check points we expect to pass are:

(a) Start layout of all boards for engineering model.

(b) Start layout of model pallets.

(c) Start building boards for engineering models.

3. ANTENNA SUBSYSTEM

3.1 ANALYSIS AND MODEL STUDY

3.1.1 Analysis

A previous section has discussed the trade-offs obtainable in the symetrical vs. the asymetrical antenna arrangement. As an independent check, because this work is rather tedious and subject to error, the antenna coverage was run on a digital computer. The results of the two approaches are in close agreement, showing that the designed coverage is obtained more easily with the .5 λ asymetrical spacing and the ambiguity problem is greatly minimized.

3.1.2 Model Study - Traveling Wave Antenna

The ground illumination requires two line sources of about 18 ft. length on the under side of the vehicle. This can be accomplished with a traveling wave antenna as well as the discrete resonant slot element antenna that will be discussed in the following section. As of this time, the choice has not yet been made as to which of the two will be finally used. The advantage of the traveling wave antenna is in relative simplicity, low weight and possibly in bandwidth, while the discrete element antenna is more conventional, and hence is a sure approach.

The antenna being developed is a TEM wave excited slot as in the accompanying figure 3-1. Like the lumped element model, the width is greatly restricted by space available, making the slots far from resonant. There are 40 slots per wavelength, which are tightly coupled to the total line current making it possible to get a reasonable radiation per wavelength.

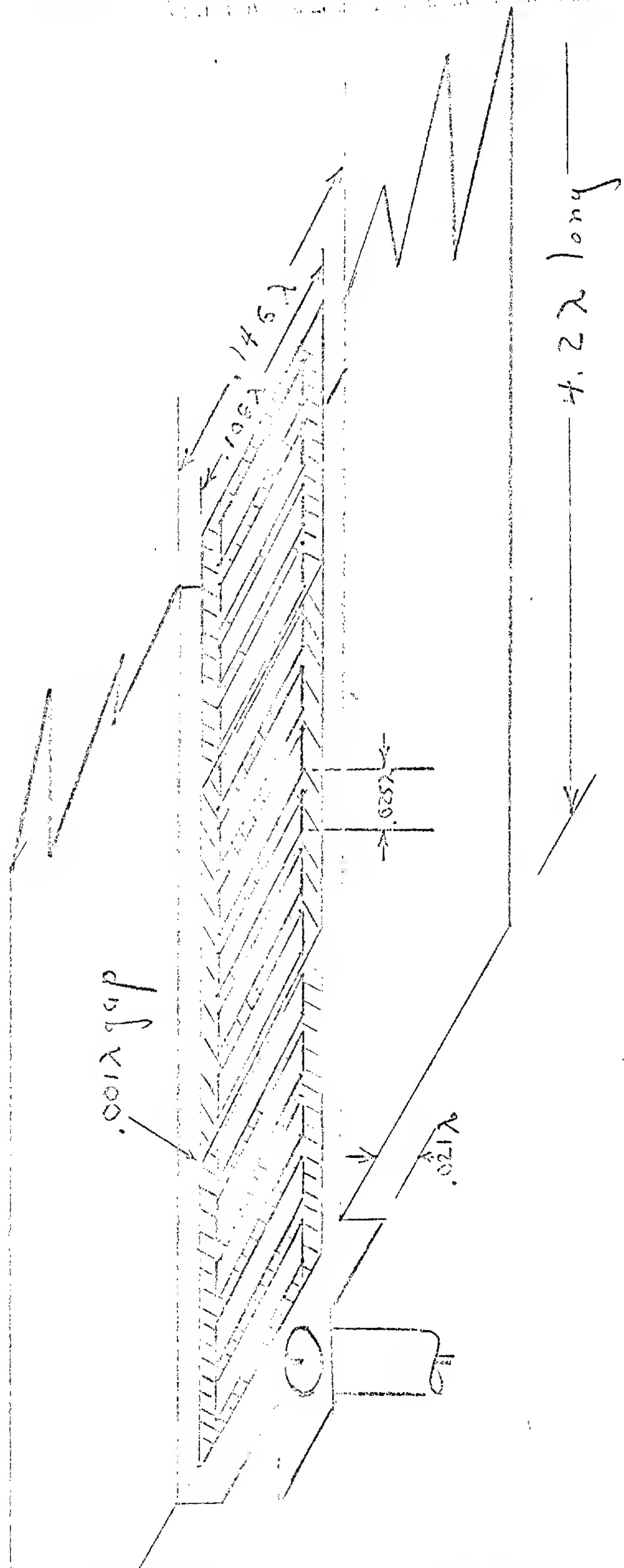

Figure 3-1 Traveling Wave Antenna

The wave velocity giving a beam as required at 30° from endfire is 115% of free space. This fast wave is achieved by a .010" cut through the ladder between each sixth gap, providing series capacity in the line. (See figure 3-1). In general it has been found easier to form a beam closer to the broadside direction. Thus the problem reduces to slowing the wave down sufficiently to give the correct pointing direction, and to simultaneously achieve high gain and low side lobes. The closest that has been realized to this time is about 6 db gain at 34° from end fire with 10 db side lobes.

3.1.3 Plans for Next Reporting Period, Analysis and Model Study

This radiation is now far enough along that it can be used to model the complete antenna, both in the 1 λ and the 1/2 λ transverse separation configuration. This will be done at 4 to 1 scale frequency which is the ratio being used for the present work. This rather complete model will give conclusions which are about equally valid for the lumped element type of antenna and for the traveling wave type of antenna. A final step in the modeling work will be to tilt the slot radiators to compensate for the 18° tilted plane on which they are mounted.

3.2 DEVELOPMENT OF ELEMENTS AND POWER DIVIDERS

Hardware development and layout for a full scale feasibility discrete element demonstration antenna is nearly complete. This antenna configuration, which consists of an array of radiating elements fed from power dividers cascaded

on a single transmission line, is compatible with space allocation in the vehicle. Phase control of the radiating elements will be achieved by the length of coaxial cable coupling the radiating element to the power divider.

3.2.1 Radiating Elements

A radiating element configuration was developed having an input impedance equivalent to a single parallel resonant circuit matched to a 50 ohm line at center frequency with a 3% bandwidth for a VSWR less than 2. This bandwidth may increase in array operation due to the proximity effects of the other radiators. If a further bandwidth increase is necessary, it may be achieved by coupling the radiator input to a resonator through a quarter wave line, producing the equivalent of a two stage filter.

3.2.2 Power Dividers

The power dividers being designed are directional couplers utilizing a pair of enclosed, continuously coupled, quarter wave long conductors. These power dividers are located adjacent to the corresponding radiating element and occupy a one inch square cross-section.

3.2.3 Plans for Next Reporting Period, Elements and Power Dividers

The design of radiating elements and power dividers for a full scale demonstration antenna will be completed and released for fabrication.

3.3 FABRICATION AND TEST OF DELIVERABLE ANTENNA SYSTEM

No fabrication releases have yet been made in this area.